UNIVERSITÀ DEGLI STUDI DI CAGLIARI

PhD Programme

Molecular and Translational Medicine

Cycle XXXI

Department of Biomedical Sciences

Unit of Oncology and Molecular Pathology

THYROID HORMONE AND METABOLIC REPROGRAMMING IN HEPATOCELLULAR CARCINOMA

Scientific Disciplinary Code: Med/04

PhD student Lavinia Cabras

PhD Programme coordinator Prof. Amedeo Columbano

Tutor Prof. Amedeo Columbano

Final exam 2018-2019

ACKNOWLEDGEMENTS

I would like to express my sincere gratitude to Professor Amedeo Columbano and Professor Giovanna Maria Ledda for giving me the chance to carry out my PhD in their laboratory. They also enabled my scientific and intellectual development paralleled by precious experiences. Their support was never lacking, even when I was abroad, and it was fundamental for my training.

My sincere thanks go to Dr. Mariano Barbacid for giving me the opportunity to join the Experimental Oncology group at CNIO in Madrid and Dr. Carmen Guerra for her guide and support during that period. I thank all the Madrid group for making me feel like home since the first day, for their scientific help, but especially for their positive attitude that I promised to keep with me. A special thank goes to Mari Carmen Lechuga for her help, without her my project there would not have been possible. I am very grateful to Teresa and Magdi for their precious teaching and the work done together. A particular thank goes to Fer, Laura and Marina for sharing this part of our lives together and for being the friends I would have hoped to find in this experience. I will never forget all these friends and the beautiful moments spent with them.

My gratitude also goes to Professor Silvia Giordano from IRCCS of Candiolo and Dr. Andrea Rasola and Dr. Carlos Sanchez-Martin from the University of Padova for accepting me in their laboratories, contributing to my scientific education during this period.

I also would like to thank Dr. Marta Kowalik for her significant help and contribution to the work presented in this thesis and Prof. Andrea Perra for his constant help whenever I needed it.

I am also sincerely grateful to Dr. Vera Leoni and Dr. Pia Sulas for the contribution they have given to the present work, but especially for their constant and warm presence, being during these years a refuge for difficult moments and the perfect company for the better ones.

I would like to thank Dr. Gabriella Simbula, Dr. Monica Pibiri and Dr. Roberto Loi for their support and presence.

I am also sincerely grateful to my lab mates Sandra, Elisabetta, Claudia and Marina for their contribution to the present work, but especially for our mutual unfailing support and the capacity to understand every situation. Thank you for all the moments shared together in and out of the lab, for your patience, for our scientific conversations and our laughs.

TABLE OF CONTENTS

ABBREVIATIONS

2-AAF	2-acetylaminofluorene
2HG	2-hydroxyglutarate
ACSS2	acyl-coenzyme A synthetase short-chain family member 2
AFB1	aflatoxin B1
ATP	adenosine triphosphate
ATPase	adenosine triphosphatase
CS	citrate synthase
DAB	3.3'-diaminobenzidine
DENA	diethylnitrosamine
DIO	deiodinase
EMT	epithelial-mesenchimal transition
EPF	early pre-neoplastic foci
FADH2	flavin adenine dinucleotide
FBP	Fructose-1,6-bisphosphate
FDA	food and drug administration
FDH	fumarate hydratase
G6P	glucose-6-phosphate
G6PD	glucose -6-phosphate dehydrogenase
GGT	gamma glutamyl transpeptidase
GLS	glutaminase
GLUT1	glucose transporter 1
GST-P	placental form of glutathione-S-transferase
HBV	hepatitis B virus
HCC	hepatocellular carcinoma
HCV	hepatitis C virus
HIF1	hypoxia inducible factor 1
HK2	hexokinase 2
HRP	horseradish peroxidase
IDH	isocitrate dehydrogenase
KRT-19	cytokeratin-19

MCTs	monocarboxylate transporters
NADH	nicotinamide adenine dinucleotide
NADPH	nicotinamide adenine dinucleotide phosphate
NBT	nitro blu tetrazolium
NQO1	NAD(P)H:quinone oxidoreductase 1
NRF2	nuclear factor erythroid 2–related factor 2
OXPHOS	oxidative phosphorylation
PBS	phosphate buffered saline
PFK	phpsphofructokinase
PH	partial hepatectomy
PKM2	Pyruvate kinase M2
PPP	pentose phosphate pathway
SDH	succinate dehydrogenase
SHARP	sorafenib HCC assessment randomized protocol
T3	3,5,3’-triiodo-L-thyronine
T4	3,5,3’,5’-tetraiodo-L-thyronine
TALDO1	transaldolase 1
TCA	tricarboxylic acids
TH	thyroid hormone
THR	thyroid responsive elements
TIGAR	TP53-induced glycolysis and apoptosis regulator
TKT	transketolase
TREs	thyroid hormone receptors
TRH	thyrotropin-releasing hormone
TSH	thyroid stimulating hormone

ABSTRACT

Hepatocellular carcinoma is the fourth leading cause of cancer-related death worldwide. Despite new molecular-targeted therapies have been approved, the benefits that can be obtained from the current therapies remain still disappointing. Thus it is mandatory to find more efficient and powerful therapeutic solutions for this aggressive tumor. Recent studies reveal a condition of local hypothyroidism characterizing HCC from pre-neoplastic lesions till fully developed HCCs. Accordingly, a short treatment with thyroid hormone (T3) caused the regression of pre-neoplastic lesions in a rat model of hepatocarcinogenesis. Moreover, several recent studies have shown the capacity of T3 of inducing mitochondrial metabolism, suggesting a role of T3 in modulating Warburg phenomenon. Based on these evidences and our preliminary results, we hypothesized that T3 may interfere on HCC development through a reversion of the metabolic reprogramming of pre- and neoplastic hepatocytes.

The first aim of the present study was to investigate whether the observed T3-dependent regression of pre-neoplastic nodules is due to its capacity to revert the Warburg phenotype of pre-neoplastic hepatocytes. Transcriptomic analysis showed that a short T3 administration caused a shift of the metabolic profile of the aggressive pre-neoplastic nodules towards that of the normal liver. This effect preceded the regression of the nodules and was associated to global reduction of G6PD expression and restoration of SDH activity.

Since the diagnosis of human HCC is often made at late stages, we investigated whether T3 could exert its anti-tumorigenic effect also on fully developed HCCs and if this effect was associated to a reversion of the metabolic reprogramming of cancer cells. First of all, we found that HCCs, despite down-regulation of the T3/TR axis were able to respond to a brief treatment with T3 and showed evidence of a return to a normal metabolic profile. Moreover, treating HCCs-bearing rats with repeated cycles of T3, we observed a significant decrease of tumor burden accompanied by a restoration of a normal metabolic profile. This was evaluated by analysis of several enzymes involved in glycolysis, pentose phosphate pathway and mitochondrial respiration known to be altered in HCCs.

Finally, we wondered whether following withdrawal of T3 the anti-tumorigenic effect of this hormone could be maintained. Interestingly, 4 weeks after T3 withdrawal, rats previously treated with T3 did not show any increase of tumor burden.

Taken together, these results suggest that T3 exerts an important anti-tumoral effect at early and late stages of HCC development and one of the mechanisms responsible for this effect could be its capacity to revert the metabolic reprogramming characterizing these lesions. They also suggest that recently developed T3 analogs, devoid of T3 negative side effects, might represent a promising tool in human HCC therapy.

ABSTRACT

Il carcinoma epatocellulare (HCC) rappresenta la quarta causa di morte al mondo per cancro ed è caratterizzato da una prognosi infausta anche per l'inefficacia delle attuali terapie. Emerge, dunque, l'esigenza di sviluppare nuove e più adeguate soluzioni terapeutiche. Studi recenti hanno dimostrato che una condizione di ipotiroidismo locale caratterizza il processo di epatocancerogenesi, a partire dalle iniziali lesioni pre-neoplastiche fino allo stadio di HCC. Conseguentemente, un trattamento di 7 giorni con l'ormone tiroideo (T3) causa una riduzione del 70% del numero dei noduli pre-neoplastici generati utilizzando un modello animale di epatocancerogenesi. Sulla base del noto effetto della T3 sull'attività mitocondriale e della riprogrammazione metabolica caratterizzante le lesioni pre- e neoplastiche epatiche, abbiamo ipotizzato che la T3 potesse esercitare il suo effetto anti-tumorale interferendo sulla loro riprogrammazione metabolica.

Il primo obiettivo del presente studio è stato valutare se la regressione dei noduli pre-neoplastici indotta da T3 fosse dovuta alla sua capacità di riportare il fenotipo Warburg degli epatociti pre-neoplastici al normale profilo metabolico. L'analisi dell'espressione di geni associati al metabolismo ha mostrato che la somministrazione di T3 è in grado di riportare il profilo metabolico dei noduli simile a quello del tessuto di controllo. Tale effetto precede la regressione dei noduli.

Successivamente, poichè l'HCC viene generalmente diagnosticato ad uno stadio avanzato in cui non risponde efficacemente alle attuali terapie, abbiamo valutato se la T3 fosse in grado di esercitare il suo effetto antitumorale anche quando somministrata ad animali con HCC e se questo effetto fosse associato al ripristino di un normale profilo metabolico. I risultati ottenuti hanno indicato che gli HCC mantenevano la capacità di rispondere a un breve trattamento con T3, mostrando al contempo evidenze di un ritorno ad un metabolismo normale.

Il trattamento con cicli ripetuti di T3 ha causato una drastica e significativa riduzione del numero e dimensioni dei tumori, associata ad uno "switch" da metabolismo di tipo glicolitico a quello ossidativo, come valutato mediante l'analisi di enzimi coinvolti nella glicolisi, nella via dei pentoso fosfati e nella respirazione mitocondriale. Alla regressione degli HCC si accompagnava un ripristino del normale funzionamento dell'asse T3/TR.

Infine, abbiamo valutato se l'effetto antitumorale, osservato dopo 5 cicli di T3, venisse mantenuto anche riportando gli animali ad una dieta normale. Sorprendentemente, 4 settimane dopo la sospensione del trattamento con T3 non si evidenziava alcun aumento nella percentuale di tumori, dimostrando la persistenza dell'effetto antitumorale della T3.

Complessivamente, questi risultati evidenziano un potente effetto antitumorale del T3, esercitato sia in stadi precoci che tardivi nello sviluppo dell'HCC e suggeriscono che la capacità di riportare alle condizioni normali il metabolismo Warburg, tipico delle cellule cancerose, rappresenti un meccanismo rilevante in tale processo. L'utilizzo di tiromimetici recentemente sviluppati e privi degli effetti collaterali dell'ormone, potrebbe rappresentare uno strumento promettente nella terapia dell'HCC umano.

INTRODUCTION

Metabolic reprogramming as a hallmark of cancer

Cancer occurs through a multistep process in which cancer cells acquire several functional capabilities that allow them to proliferate, survive and disseminate. These cancer-associated traits have been thoroughly studied over the years leading to the identification of so-called "hallmarks of cancer" (Figure 1). Since the original publication, progresses made in cancer research led to revisit and include new hallmarks among the original ones. The widespread applicability of the concepts expressed in the Hanahan and Weinberg's work provided a powerful help in developing new therapeutic approaches as drugs that interfere with some of the 'hallmarks of cancer' have been already generated, are in clinical trials and, some of them have been approved for clinical use [1].

Metabolic reprogramming of cancer cells has been introduced among the hallmarks of cancer only in the last decade. Cancer cells adjust energy metabolism in order to support continuous cell growth and proliferation. In particular, neoplastic cells display increased ability to acquire the nutrients they need, then moving them to metabolic pathways that contribute to tumorigenic properties. These alterations are supposed to be both direct and indirect consequence of oncogenic mutations, and together take part in the maintenance of the tumorigenic state [2].

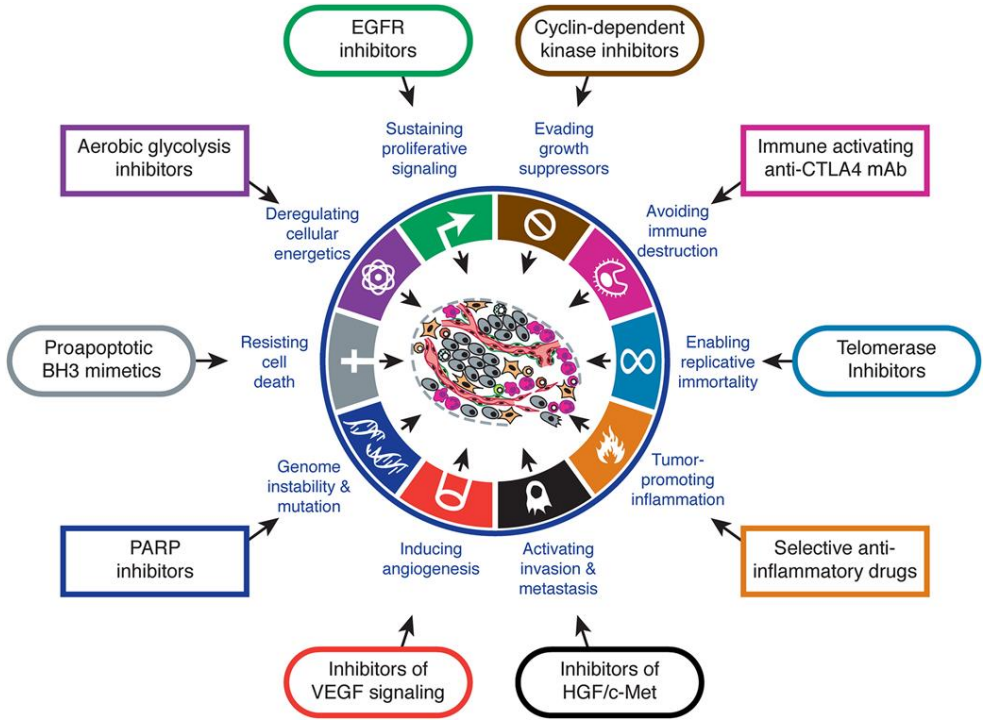

Figure 1 . Illustration of the "hallmarks of cancer" and relative therapeutic strategies [1].

The “Warburg effect”

Altered cancer metabolism has become a topic of renewed interest in the last decade, but the first observations on metabolic alterations of cancer cells were made nearly a century ago by the German physiologist Otto Warburg. Under aerobic conditions, normal cells process glucose first to pyruvate in the cytosol and then to carbon dioxide in the mitochondria; when oxygen is limiting or not available, under anaerobic conditions, glycolysis is favoured and very little pyruvate is diverted to mitochondria, while the major part of pyruvate is “fermented” into lactate. It was Warburg to observe for the first time an anomalous characteristic of cancer cell energy metabolism: even in presence of oxygen, most cancer cells tend to convert the majority of glucose into lactate using only glycolysis for glucose-dependent adenosine triphosphate (ATP) production, leading to a state termed “aerobic glycolysis”, also known as “Warburg effect”. A first explanation for Warburg’s observation was that cancer cells develop mitochondrial defects that impair aerobic respiration leading the cells to rely on glycolysis for energy production [3–5]. However, several works reported that mitochondrial function is not impaired in most cancer cells, suggesting the existence of another explanation for aerobic glycolysis in tumor cells [6,7]. Moreover, considering that only 2 molecules of ATP per molecule of glucose are produced through the aerobic glycolysis, whereas glycolysis coupled to oxidative phosphorylation (OXPHOS) generate up to 36 ATP per molecule of glucose, a functional rationale for aerobic glycolysis still remains elusive (Figure 2).

Among possible explanations for such a metabolic switch, it was proposed that inefficient ATP production is a problem only when there is poor supply of nutrients. However, this situation does not regard cancer cells, that display a strong up-regulation of glucose transporters, leading to increased glucose uptake [8]. In fact, most cancer cells exhibit a glycolytic activity that is estimated to be even 200-fold higher than that of normal cells [9]. Therefore, increased supply of glucose, along with a high rate of glycolytic activity, lead to an increased ATP production even in conditions of “aerobic glycolysis”.

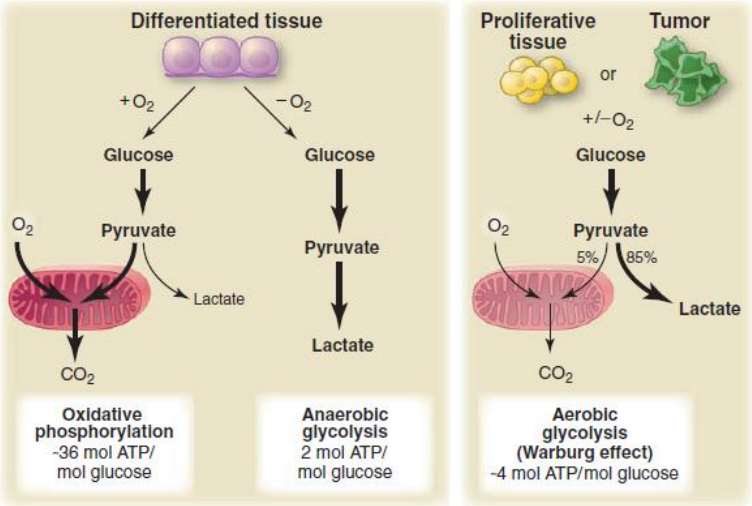

Figure 2 . Illustration of the differences in energy production between oxidative phosphorylation, anaerobic glycolysis and aerobic glycolysis [10].

Another possible reason is that cells, that continuously proliferate, have requirements that extend beyond the only need to produce ATP. To generate a new cell, nucleotides, amino acids and lipids are needed. In normal conditions one molecule of glucose can generate up to 36 ATP, but only 2 Nicotinamide Adenine Dinucleotide Phosphate (NADPH) through the Pentose Phosphate Pathway (PPP) and 6 carbons. It has been observed that to produce amino acids and nucleotides a cell needs more equivalents of carbon, to build the molecular skeleton, and NADPH as reducing power for a wide variety of biosynthetic reactions, rather than ATP. From this point of view it is clear why most cancer cells down-regulate mitochondrial respiration in favour of aerobic glycolysis: converting all the glucose to CO_2 via OXPHOS to maximize ATP production, will result in a loss of carbons that are needed. Indeed, citrate from the Tricarboxylic Acid Cycle (TCA cycle) could be used for fatty acids synthesis, while glycolysis intermediates for amino acids and ribose for nucleotides [10] In addition, TCA cycle is the major negative regulator of glucose metabolism, so the conversion of glucose in lactate prevents a feedback repression of glycolysis by excess ATP produced by mitochondria [2].

Irrespectively of the reasons underlying this metabolic reprogramming, altered cancer metabolism has been described in many cancer types, such as lung, liver and pancreatic cancer [11–13].

Cancer cells exhibit enhanced uptake and utilization of glucose and glutamine

As abovementioned, in order to sustain the need of new macromolecules to support continuous proliferation, most cancer cells increase the import of nutrients from the environment, mainly glucose and glutamine (Figure 3). Catabolism of glucose and glutamine provides carbon intermediates that serve as building blocks for the synthesis of new molecules. In parallel, controlled oxidation of carbons derived from glucose and glutamine, allows to store their reducing potential in form of Nicotinamide Adenine Dinucleotide (NADH), Flavin Adenine Dinucleotide ($FADH_2$) and NADPH. NADH and $FADH_2$ mediate the transfer of electrons through the electron transport chain which culminates in ATP production, while NADPH provides reducing power for biosynthetic reactions and contributes to maintain cellular redox capacity. Apart from carbon, glutamine provides nitrogen required for biosynthesis of purine and pyrimidine nucleotides and non-essential amino acids. Moreover, intracellular glutamine plays a role in acquisition of essential amino acids through the antiporter L-Type Amino Acid Transporter 1 (LAT1), further contributing to the needs of a proliferating cell [14].

Since in normal conditions nutrients uptake is strictly regulated by growth factors and adhesion inputs, the ability to internalize high quantities of glucose and glutamine is an exclusive characteristic of cancer cells. Indeed, tumor cells acquire a significant degree of independence from external signalling, as a consequence of oncogenic alterations that accumulate during cancer progression [15]. Deregulated phosphatidylinositide 3-kinases/Akt (PI3K/Akt) signalling pathway occurs in many cancers and has been shown to be a master regulator of glucose uptake and utilization, promoting the expression of the type I glucose transporter (GLUT1) and translocation of GLUT1 protein to the cell surface [16,17]. Up-regulation of GLUT1 and increased glucose

consumption have been shown to depend also on Ras pathway, constitutively activated in many cancers [18]. Moreover, Akt enhances the activity of Hexokinase 2 (Hk2), the first enzyme of glycolysis that prevents [19], and potentiates the activity of phosphofructokinase (PFK), the enzyme that catalyses a key irreversible step of glycolysis, thus allowing the flux through glycolysis [20]. Regarding glutamine, the principal driver of glutamine uptake and utilization is the transcription factor c-myc, upregulated in proliferating cells [21]. C-myc induces the transcription of glutamine transporter ASCT2 and SN2, promoting at the same time the expression of enzymes involved in glutamine utilization, such as Glutaminase 1 (GLS1) and CAD, that convert glutamine to glutamate. Glutamate can alternatively fuel the TCA cycle entering as α-ketoglutarate or contributing to amino acids synthesis [22,23].

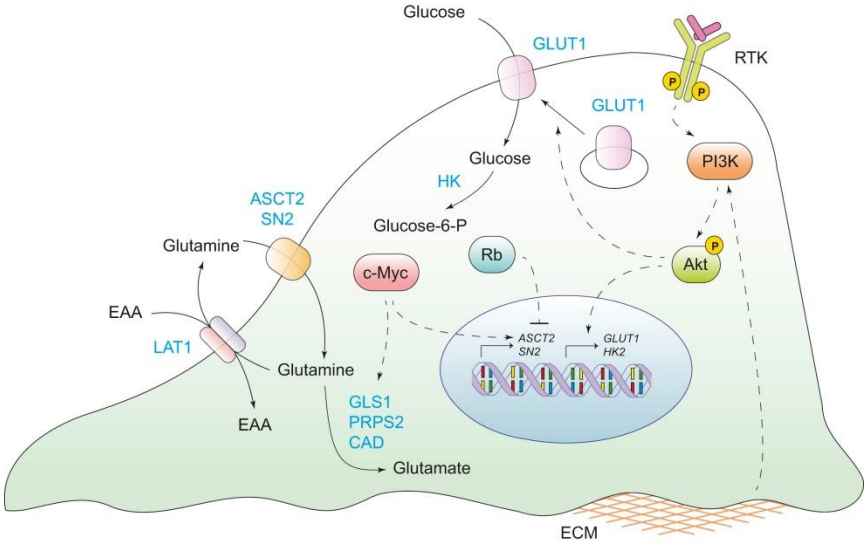

Figure 3 . Deregulated uptake of glucose and glutamine in cancer cells [2].

Mitochondrial respiration

Along with enhanced glucose and glutamine uptake, many cancer cells down-modulate mitochondrial respiration. Such down-regulation could be a consequence of increased glycolysis or an effect of oncogene activation or tumour suppressor inactivation. Inactivating mutations of genes encoding enzymes belonging to the TCA cycle, such as succinate dehydrogenase (SDH) and fumarate hydratase (FDH), have been reported [24]. These mutations promote the accumulation of succinate and fumarate that have recently been proposed as oncometabolites for their pre-neoplastic effects [25]. In fact, both succinate and fumarate can lead to hypoxia-inducible factor 1 (HIF1) stabilization that in turn promotes angiogenesis, metabolic changes and epithelial-mesenchimal transition (EMT). In addition, inactivating mutations of mitochondrial isocitrate dehydrogenase (IDH) 1 and 2 cause accumulation of another oncometabolite, 2-hydroxyglutarate (2HG). 2HG is indirectly responsible for epigenetic changes in cancer cells affecting the activity of dioxygenases, mainly histone and DNA demethylases [26]. Moreover, inactivating mutations of genes encoding respiratory complex subunits have been reported in several tumors [27–29].

Cancer cells divert metabolic intermediates into biosynthetic pathways

To support the increased biosynthetic demand, cancer cells change the way nutrients are used once they are internalized into the cell. Along with enhanced glycolysis and down-regulated mitochondrial respiration, many intermediates of glycolysis and TCA cycle can be diverted into other pathways, thus generating biosynthetic precursors (Figure 4).

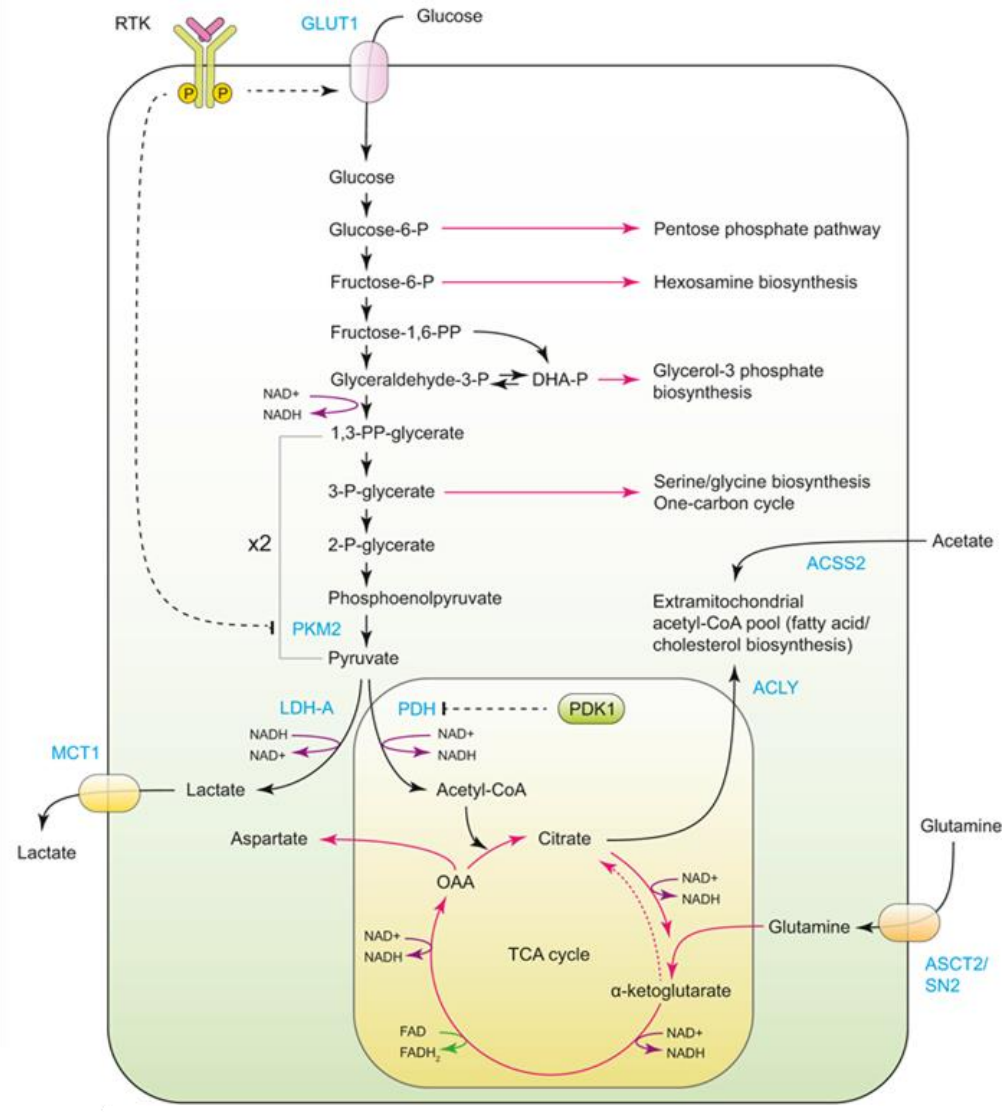

Figure 4 . Diversion of glycolysis and TCA cycle intermediates for biosynthesis [2].

Not surprisingly, the rate-limiting enzymes within branching pathways of glycolysis are frequently up-regulated in tumors. Glucose-6-phosphate (G6P) from glycolysis is diverted into the PPP that generates NADPH and Ribose-5-phosphate, a structural component of nucleotides. Indeed, the PPP often results up-regulated in many tumor types, including breast, cervical, liver, lung, colon and gastric cancer [30]. In particular, glucose-6-phosphate dehydrogenase (G6PD), the rate-limiting enzyme of the oxidative branch of the PPP, is often up-regulated in terms of expression and

activity. Key enzymes of the non-oxidative branch of the PPP, such as Transketolase 1 (Tkt1) and transaldolase 1 (TALDO1) are also frequently up-regulated [31,32].

Among the other glycolytic intermediates, glycerol-3-phosphate can be used for synthesis of phospholipids, structural components of cellular membranes, while 3-phosphoglycerate is used to generate serine [2]. Serine is the major contributor to the folate cycle, whose intermediates are recycled for synthetizing purines and thymidine. In addition it has been recently shown that oxidative reactions of this cycle produce up to 50% of all cellular NADPH [33]. Diversion of glycolysis intermediates into biosynthetic pathways is also favoured by TP53-induced glycolysis and apoptosis regulator (TIGAR)-dependent down-regulation of the second part of glycolysis. TIGAR, which was discovered through microarray analysis of gene expression following the p53 activation is highly conserved through vertebrate species and shares similarities with the glycolytic enzyme phosphofructokinase-2/fructose-2,6-bisphosphatase (PFK-2/FBPase-2) [34]. TIGAR, degrades intracellular fructose-2,6-bisphosphate (F-2,6-P2), which is a powerful activator of phosphofructokinase-1 (PFK-1). As a consequence of lowering F-2,6-P2 levels, TIGAR decreases the activity of PFK-1 and therefore reduces glycolytic flux (Figure 5). TIGAR expression results significantly up-regulated in many human cancers, for example breast cancer, colorectal cancer. Among the most important consequences of TIGAR activity is a diversion of the glycolytic metabolites to alternative metabolic fates, such as the hexosamine pathway to support glycosylation and first of all, to the oxidative or non-oxidative branches of the PPP [35]. Moreover, enhanced activation of TIGAR results in a decrease of fructose-1,6-bisphosphate (FBP), that acts as activator of pyruvate kinase M2 (PKM2), the predominant pyruvate kinase isoform in HCC cells [36]. Several agents promote the switch to the more active tetrameric form of PKM2, such as FBP and serine, while phosphorylation, acetylation and oxidation cause the switch to the less active dimeric form [37,38]. By reducing FBP formation, the switch to the PKM2 less active form is favoured contributing to the accumulation of glycolytic intermediates that can be used for anabolic reactions.

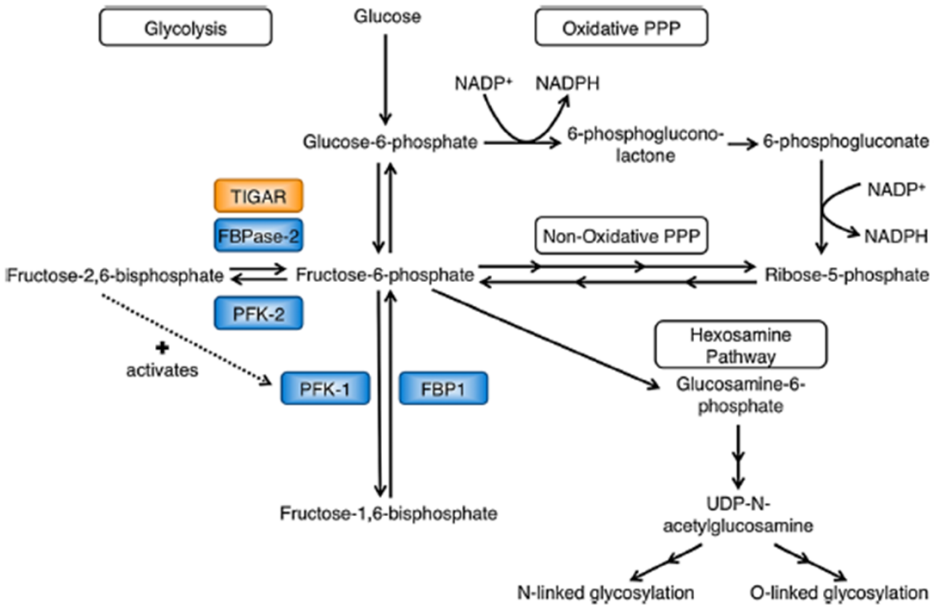

Figure 5 . Action of TIGAR in metabolic reprogramming [35].

Any excess from glycolysis, not utilized for biosynthesis, is preferentially converted into lactate, in order to preserve a sufficient pool of NAD+ to support glycolysis. Lactate is excreted out of the cell through the monocarboxylate transporters (MCTs), while pyruvate that does enter the TCA cycle is converted into citrate. Citrate is successively exported into the cytosol and broken down in oxaloacetate and acetyl-CoA. Oxalacetate in converted in malate and transported again to the mitochondria, while acetyl-CoA takes part in lipid biosynthesis [2]. Apart from citrate, the TCA cycle also provides precursors for non-essential amino acids biosynthesis. Actually for most cancer cells the integrity of TCA cycle intermediates often depends on glutamine supply [39]. Once entered in the cell through ASCT2 and SN2 transporters, glutamine is internalized into mitochondria in the form of glutamate and converted in a-ketoglutarate. Oxidation of α-ketoglutarate leads to generation of malate that can escape from mitochondria and in the cytosol be converted into pyruvate in a reaction that produces NADPH in a glucose-independent manner [11]. Moreover, it has been observed that many cancer cells use extracellular acetate as a source for acetyl-CoA for biosynthesis. Once internalized, acetate is converted into acetyl-CoA through a reaction amplified in many cancers types and catalysed by acetyl-CoA synthetase 2 (ACSS2), thus fuelling the TCA cycle [2].

Biochemical traits related to metabolic reprogramming have been found in almost all types of tumors with characteristics varying among different types of cancers. Hepatocellular carcinoma (HCC) represents one of the most important examples of the reprogramming of glucose metabolism. [40]. Since HCC represents a global health challenge, due to its rising incidence, low survival rate and advanced stage diagnosis, identification of metabolic features that contribute to HCC progression could be helpful for the identification of new therapeutic strategies.

Hepatocellular carcinoma

Primary liver cancer is the sixth most common cancer in the world [41]. Approximately 850,000 new liver cancer cases and 800,000 deaths are registered per year [42]. HCC represents about 90% of all cases of primary liver cancer and is the fourth leading cause of cancer-related deaths worldwide [43]. The vast majority of HCCs occur in sub-Saharan Africa and Eastern Asia, with China alone accounting for more than 50% of the world's burden [44] (Figure 6). Intermediate incidence rates occur in countries of the Central Europe, while for Northern Europe, Middle East, Oceania and America the lowest incidence rates are registered [45].

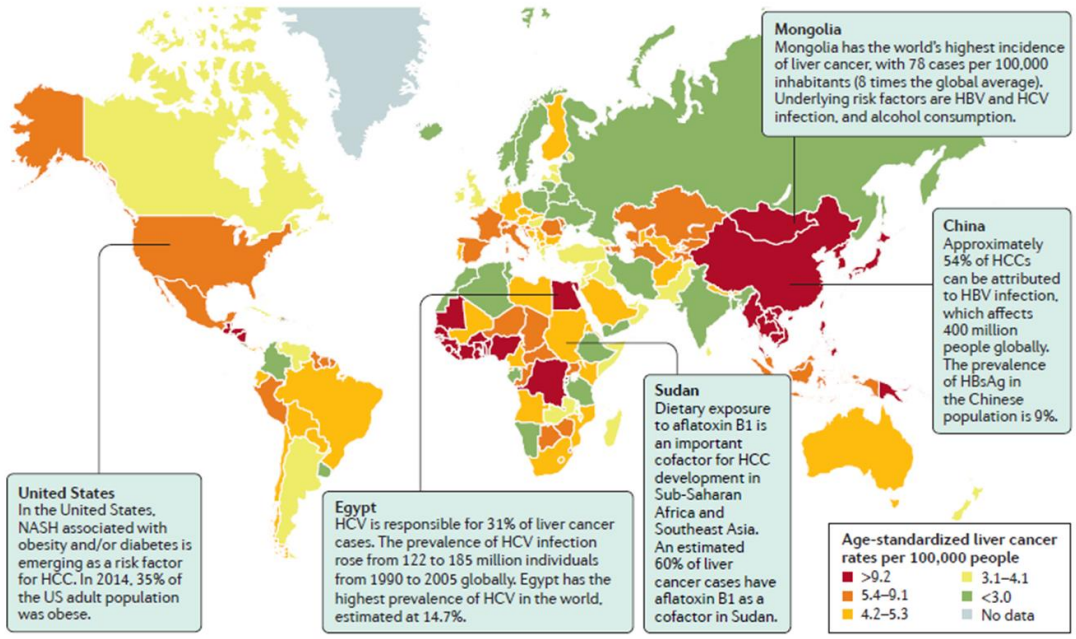

Figure 6 . Incidence of HCC and main risk factors [42].

Regions with high and low-rate incidence of HCC are characterized by a prevalence of different risk factors for HCC. Hepatitis B virus (HBV) infection and consumption of Aflatoxin B1 (AFB1)-contaminated food are the major risk factors in high-rate regions, such as Asia and Africa. In contrast, major risk factors in low-rate areas are Hepatitis C virus (HCV) infection, alcohol consumption, obesity, diabetes and metabolic syndrome [44].

Natural history of HCC

Hepatocellular carcinoma develops through a multistep process that arises from a chronic liver disease characterised by inflammation and fibrosis. Observations of patients affected by conditions that represent well-known risk factors for HCC show a variability in the window of time from the exposure to the occurrence of HCC. Studies on HCV-infected patients suggest that the development of HCC requires about 10 years from the diagnosis of cirrhosis and 30 from the exposure to the virus [46]. Interestingly, in the case of HBV-derived HCC, the time course is less predictable, since HCC may precede the occurrence of cirrhosis [47].

Recent advances in liver cancer research allows to understand the natural history of HCC, through the identification of three distinct phases between the initial biological changes that characterize the disease and the patient's death (Figure 7).

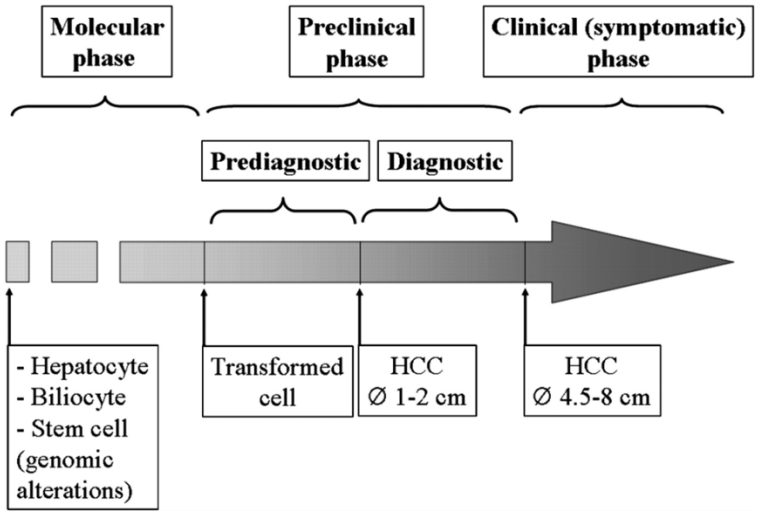

Figure 7 . Schematic representation of the different phases of HCC natural history [48].

During the "molecular phase", conditions like inflammation, regenerative response to cell loss and the action of viral proteins drive an enhanced expression of cytokines and growth factors. As a consequence, cells undergo mitogenic stimulation due to exposure to elevated levels of growth factors. This pre-neoplastic phase includes the sequential genomic alterations leading to cell transformation. Mechanisms of cellular transformation differ depending on the cell type. Differentiated cells (hepatocytes and cholangiocytes) acquire a growth advantage by enhanced proliferation and inhibition of apoptosis, while genetic alterations of stem cells interfere with the differentiation process. Alterations of genes slowly develop during this phase producing the malignant hepatocyte phenotype and significantly increase in dysplastic and neoplastic hepatocytes leading to several molecular variants of HCC [48].

In the "preclinical phase" there is an initial period in which dysplastic foci are still too small to be detected by imaging techniques (diameter < 1mm). When they reach 1-2 cm of diameter ("diagnostic phase"), they are still asymptomatic, but they can be detected because of their burden.

However, in this phase they still lack invasive patterns, such as microvascular invasion and extrahepatic spread [48,49].

In the “clinical” or “symptomatic phase” the degree of liver dysfunction and the tumor burden lead to the clinical presentation of HCC. In patients with chronic liver disease, HCC usually becomes symptomatic when it reaches 4.5-8 cm of diameter [50]. The most common presenting symptoms in a cirrhotic liver are hepatomegaly, abdominal pain, ascites and constitutional syndrome. However, HCCs-arising in a non-cirrhotic liver are usually constituted by big solitary masses exhibiting a fast and infiltrative growth with vascular invasion and metastases [51].

Unfortunately, HCC is often diagnosed at an advanced stage when it is not amenable to curative treatments and death occurs within few months. Indeed, patients with advanced HCC have a survival rate of 0-10% [52]. Conversely, early-stage HCC lesions are not so extended and are frequently curable, so that these patients are characterized by a 5-year survival rate of 50%. These data led to the development of protocols for screening and surveillance of patients at risk for HCC, such as patients affected by either HBV or HCV.

Despite an improved treatment of viral hepatitis and an increased screening of high risk patients in developed countries, only around 40% of HCC patients are eligible for potentially curative treatments (resection, transplantation, or local ablation) and 20% for chemoembolization. Around 40% of patients are diagnosed with advanced disease [42] and thus, systemic therapy is indicated for a considerable proportion of patients. The major problems in developing effective therapies for HCC involve the intrinsic chemoresistance of HCC, the pharmacologic problems due to the presence of a diseased liver and the very advanced stage of diagnosis. Unfortunately, the efficacy of traditional chemotherapeutic agents and their ability to produce a significant survival benefit is questionable.

In 2005, the Food and Drug Administration (FDA) approved the multikinase inhibitor Sorafenib for the treatment of unresectable HCC [53]. However, the Sorafenib HCC Assessment Randomized Protocol (SHARP) trial showed an increase in survival among patients with advanced-stage disease of only 3 months [54].

More recently, Regorafenib, another multikinase inhibitor, has been approved as a second-line therapy for HCC [55]. Although a recent study [56] reported an improvement of the overall survival in patients who were subjected to a treatment with the sequence of Sorafenib followed by Regorafenib, the results are still far from being satisfactory.

The lack of more effective therapeutic strategies reveals the need of studies aimed to the identification of new target pathways, leading to the development of more effective compounds. Moreover, understanding the mechanisms underlying tumor growth may lead to identify new markers to improve HCC early diagnoses, that would greatly improve patients’ survival.

Metabolic characteristics of HCC

Identification of alterations that distinguish tumor cells from functionally normal hepatocytes might result helpful in identifying new targets for HCC therapy. Metabolic gene networks have been shown to be heterogeneous in all types of cancer, including HCC [57]. The study of the expression of 2761 metabolic genes in 521 human HCC by Nwosu *et al*. reported that numerous metabolic genes were deregulated regardless of the etiological background of the different groups of patients. Among the most up-regulated metabolic genes were those involved in glycolysis, PPP, TCA cycle, nucleotide biosynthesis, glucose and glutamine transporters and lipid biochemistry, as reported in Figure 8. Moreover, proteomics analyses revealed that more than 90% of those genes were significantly expressed in the same direction as found at gene level [12].

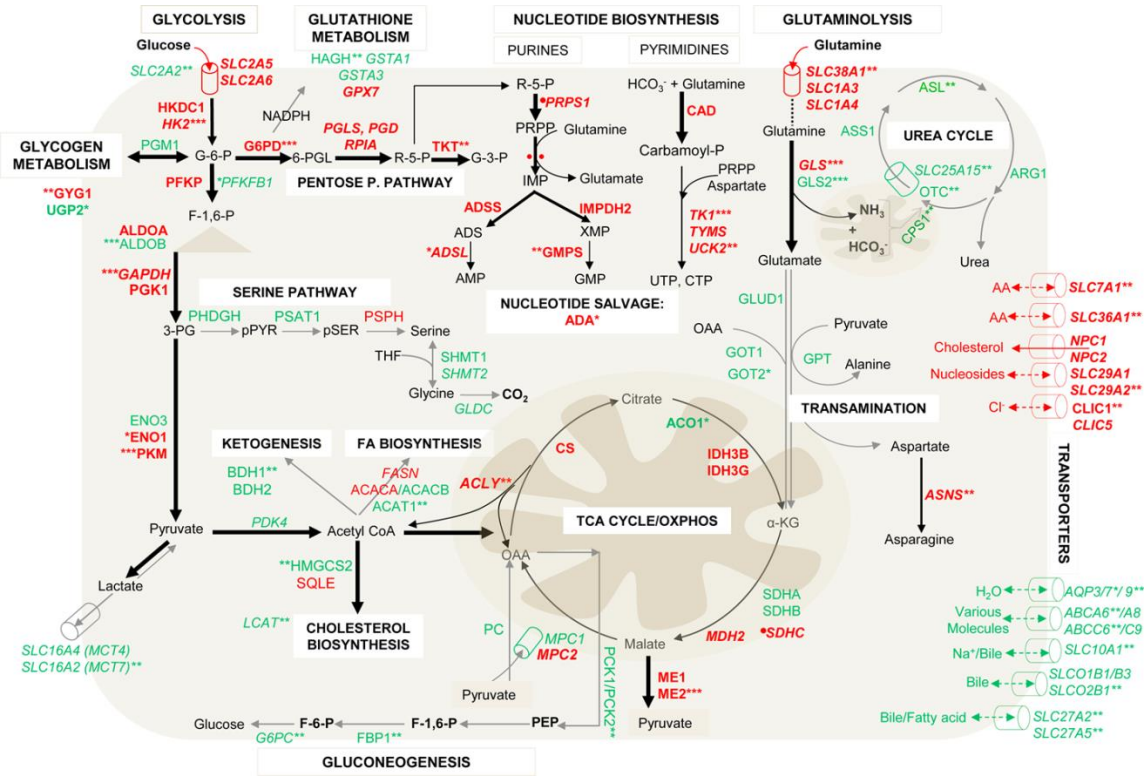

Figure 8 . Deregulated metabolic genes in human HCC [12].

A metabolic reprogramming in HCC has been also extensively studied in animal models of hepatocarcinogenesis. Up-regulation of the PPP was found in several rat models of HCC [58,59]. Genetically engineered mouse models have been used for better understanding the interconnection between oncogene expression and the metabolic features of HCC [60,61]. A recent study by Kowalik *et al.* showed that the metabolic alterations found in HCC, such as enhanced glycolysis and lactate production accompanied by down-regulation of OXPHOS, occur already at early stages of cancer development. Indeed, a subset of pre-neoplastic lesions displayed enhanced expression of Glucose-6-Phosphate Dehydrogenase (G6PD), the rate-limiting enzyme of the PPP and decreased activity of succinate dehydrogenase (SDH), the complex II of the respiratory chain. Moreover, these

metabolic features were unique to the most aggressive pre-neoplastic lesions, indicating a crucial role of metabolic reprogramming in driving and sustaining the tumorigenic process [62].

Animal models of HCC: The Resistant Hepatocyte model (RH)

The late-stage diagnosis, that in most of the cases characterizes human HCC, makes the tumors hard to be clinically classified because of the intratumoral heterogeneity, that is typical of advanced stages of the disease. Since studies on initial HCC stages in humans are hampered by the clinical difficulty of diagnosing early lesions, experimental models allowing us to dissect the several steps of HCC are mandatory.

Several rodent models of HCC have been developed over the years, contributing to the current knowledge about HCC. Among these models, the Resistant Hepatocyte (RH) rat model, developed in 1977 by Solt and Farber [63], offers the possibility to identify distinct type of lesions (pre-neoplastic foci, pre-neoplastic nodules, early and fully developed HCCs) at well-defined timings.

According to this protocol, tumors are initiated by a single dose of a chemical carcinogen diethylnitrosamine (DENA), followed by a promoting regimen consisting of 2 weeks of 2-acetylaminofluorene (2-AAF)-supplemented diet, a selective inhibitor of hepatocyte proliferation, combined with partial hepatectomy (PH), a powerful growth stimulus. In these conditions only DENA-initiated cells undergo proliferation, giving rise to early pre-neoplastic foci (EPF), small spherical lesions consisting of 15-100 hepatocytes. EPF can be identified already 7 days after PH by positivity for the placental form of the enzyme glutathione-S transferase (GST-P), whose expression is normally very low in healthy adult liver [63,64].

Successively, foci progress to a nodular stage giving rise to pre-neoplastic nodules macroscopically visible on the surface of the liver and occasionally protruding from under the capsular surface [63]. During the following weeks, along with progression of pre-neoplastic nodules, a remodelling process takes place continuously involving most pre-neoplastic nodules which lose the positivity for GST-P and other pre-neoplastic markers, re-acquiring a differentiated phenotype. In parallel, a minority of pre-neoplastic nodules progress to fully developed HCCs, visible 12-14 months after DENA.

Ten weeks from DENA initiation, the GST-P+ lesions can be either positive or negative for the progenitor/stem cell marker cytokeratin-19 (KRT-19). In normal liver, KRT-19 is expressed by biliary epithelial cells, while normal hepatocytes express KRT-8 and KRT-18. Since KRT-19+ HCCs are characterized by the worst clinical prognosis among all HCC subclasses, KRT-19 is considered a prognostic marker correlated with poor outcome for HCC [65,66]. Moreover, previous observation from our laboratory showed that almost all the HCCs developed in the RH protocol are KRT-19+ [67].

These data along with the observation that KRT-19+ nodules and human HCCs share a common gene expression profile, led to the conclusion that KRT-19+ hepatocytes are the progenitor cell population for HCC [68]. All these observations suggest that R-H model not only represents a

powerful tool for studying all the stages of hepatocarcinogenesis, but also its potential translational value.

Thyroid hormones (THs) and Thyroid Hormone Receptors (THRs) in HCC

Thyroid hormones, 3,5,3',5'-tetraiodo-L-thyronine (T4) and 3,5,3'-triiodo-L-thyronine (T3) are secreted by the follicular cells of the thyroid gland under control of the hypothalamic-pituitary axis. THs influence many physiological processes, such as development, metabolism, cell growth and differentiation.

The release of these hormones by the thyroid gland is regulated by the hypothalamus through the Thyrotropin Releasing Hormone (TRH) that stimulates the pituitary gland to secrete the Thyroid Stimulating Hormone (TSH). TSH, in turn, stimulates the thyroid gland to release T3 and T4 and all this process is under control of a negative feedback loop [69]. T4 is the thyroid hormone mainly secreted in the blood stream. Once transported across the cell membrane of responsive cells by specific monocarboxylate anion transporters such as MCT8 and MCT10, T4 is converted in T3 that represent the physiological active form of T4. This conversion takes place in peripheral organs, mainly liver and kidney, and is carried out by the selenoenzymes iodothyronine deiodinase I and II (Dio1 and Dio2). Dio1 operates in kidney and liver, while Dio2 has been found in pituitary, brain and brown adipose tissue. Dio1 and Dio2 catalyze the outer ring 5'-deiodination that can be viewed as the first step in the activation of the thyroid hormone T4. Conversely, type III deiodinase is responsible for thyroid hormone inactivation converting T4 in reverse T3 (r T3) and both T3 and r T3 in the inactive form 3,3'-diiodothyronine (T2). T2 is sulfo- and glucuronide-conjugated before excretion the bile [70]. TH could be re-uptaken through an enterohepatic circulation in which the intestinal flora deconjugates some of these compounds (Figure 9)

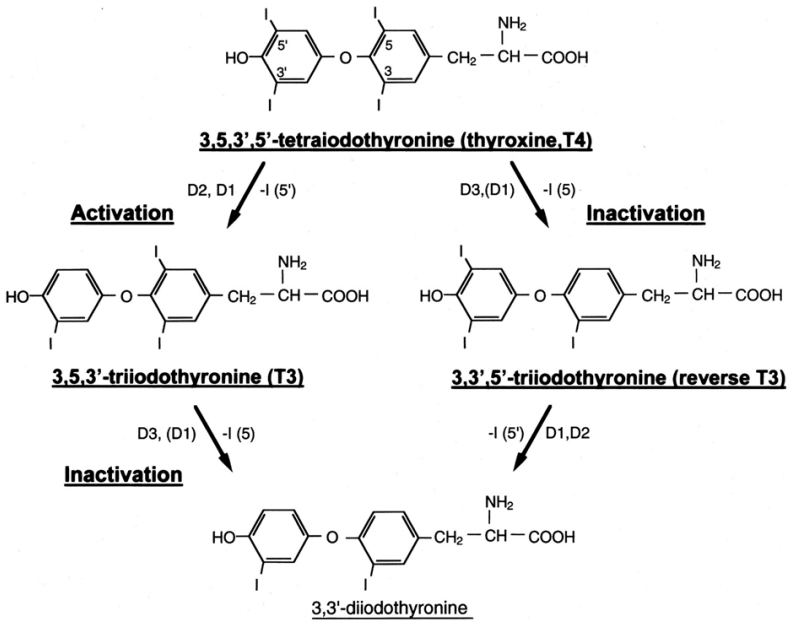

Figure 9 . Mechanisms of activation and inactivation of thyroid hormones [70].

Although it has been recently proposed the existence of non-genomic effects of T3 mediated by receptors on the plasma membrane and in the cytoplasm, the best characterized effects of THs require the Thyroid Hormones nuclear Receptors (THRs) [71]. THRs belong to the steroid/thyroid superfamily of nuclear hormone receptors which act as modulators of gene expression through their ability to recognize specific DNA sequences. THRs are encoded by two genes THRα (NR1A1) and THRβ (NR1A2) localized in human chromosomal regions 17q11.2 and 3p24.3, and rat chromosomal regions 10q3 and 15p16, respectively. The expression of THRs isoforms is tissue-dependent and developmentally regulated. THRα1 is constitutively expressed at embryonic development, and THRβ is expressed toward the later stage of development [72]. THRα1 and THRα2 are expressed at the highest levels in the brain; at lower levels in the kidneys, skeletal muscle, lungs, heart, testes, and liver. THRβ1 is expressed predominantly in the kidneys, liver, brain, heart, and thyroid. THRβ2 is mainly expressed in the brain, retina, and inner ears [73].

Several recent studies have shown the implication of THs, namely 3,5,3',5'-tetraiodo-L-thyronine (T4) and 3,5,3'-triiodo-L-thyronine (T3), and THRs in cancer. However, contradictory data do not allow to clarify whether THRs play an oncogenic or an oncosuppressor role. Many studies have reported low levels of THRs and/or altered expression and somatic mutations in several human and rodent types of cancer, suggesting that partial or complete loss of THRs function may facilitate tumor progression in breast, colon, liver, kidney, thyroid and skin cancer [74–80]. These data led to hypothesis that since THRs play a tissue-specific function, their role in cancer may vary depending on the tissue.

As to HCC, THRβ mRNA levels have been found significantly down-regulated in human and rat HCCs [80,81]. Despite an extremely high frequency of THR mutations has been reported in human HCCs [82], more recent RNAseq data from 442 human HCCs reported only two mutations for THRβ and none for THRα, suggesting that THRs mutations are not significantly involved in human HCC [82–84]. Moreover, no THR mutations were found in experimentally induced rat HCCs [80]. In addition, contrasting results have been reported about the hypermethylation status of THRs gene, thus making it difficult to clarify whether hypermethylation occurs in HCC and is responsible for the observed down-regulation of the receptor [85]. Conversely, the finding of an inverse relationship between THRβ levels and the expression of several miRNAs suggests that down-regulation of the receptor might be the consequence of regulation by miRNAs [80,86,87].

Independently of the causes of THRβ down-regulation in human and rat HCC [76,80], hypothyroidism has been indicated as a permissive factor for the development of this tumor. Indeed, Hassan *et al*. showed that women with a history of hypothyroidism had a 2.8 fold higher risk of HCC [88]. In addition, a case-control study from Reddy *et al.*, revealed that hypothyroidism was prevalent in patients with HCC of unknown aetiology [89]. Previous results from our laboratory revealed a condition of local hypothyroidism in human and rat HCCs with a decreased expression of THRs, in particular THRβ, both at protein and mRNA levels. This aspect not only characterizes fully developed HCCs, but also the most aggressive pre-neoplastic lesions indicating that sustained down-regulation of THRs may be necessary for HCC onset and progression [80]. Accordingly, a

brief T3 treatment was able to cause regression of 70% of pre-neoplastic lesions in the R-H model [90].

Based on the finding that a condition of local hypothyroid status seems to characterize both rodent and human HCCs, it is critical to investigate whether the rescue of a normal T3/THR axis by exogenous administration of T3 (a switch from a local hypothyroid to a eu/hyperthyroid status), could induce a differentiation programme not only in preneoplastic hepatocytes but also in fully transformed HCC.

AIM OF THE STUDY

Previous studies conducted in our laboratory showed that the metabolic rewiring found in rat HCC takes place since the very early stages of tumor development and specifically involves the most aggressive pre-neoplastic lesions. Our previous studies also demonstrated that a short treatment with T3 is able to induce the regression of most preneoplastic lesions.

Based on these evidences, the aim of the present study is to investigate whether:

- The observed T3-dependent regression of pre-neoplastic lesions is due to the ability of T3 to interfere with the metabolic reprogramming of these lesions.
- Fully developed HCCs retain the ability to respond to T3 administration and whether T3 is able to revert metabolic reprogramming of neoplastic hepatocytes.
- The effect of T3 on HCC growth and metabolic profile is maintained after hormone withdrawal.

MATERIALS AND METHODS

Animals

Male Fisher F-344 rats weighing 100-125 gr were obtained from Charles River (Milan, Italy). Animals have been fed a rodent standard diet (Standard Diet 4RF21, Mucedola, Milan Italy) and maintained at 25°C temperature and 12 hours light/dark daily cycle, with food and water ad libitum. The Guidelines for the Care and Use of Laboratory Animals were followed and all the animal procedures were approved by the Ethical Commission of the University of Cagliari and the Italian Ministry of Health.

Experimental protocol 1

A single dose of the carcinogen diethylnitrosamine (DENA) (Sigma Aldrich, St. Louis, MO, USA), dissolved in saline was injected intraperitoneally to rats at the dose of 150 mg/kg body weight. After a recovery period of 2 weeks, all animals were treated in accordance to the Resistant-Hepatocyte protocol of hepatocarcinogenesis [63]. Rats were fed a diet containing 0.02% 2-acetylaminofluorene (2-AAF) (Sigma Aldrich, St. Louis, MO, USA) for 1 week and then subjected to a standard two-thirds partial hepatectomy (PH) and kept for an additional week on the 2-AAF-containing diet. Five weeks after 2-AAF release, animals were randomly divided into two groups: one group was kept in basal diet (Standard Diet 4RF21, Mucedola, Milan, Italy), while the other was fed a T3-supplemented diet (4mg/kg of T3) for 2 or 4 days (Figure 10).

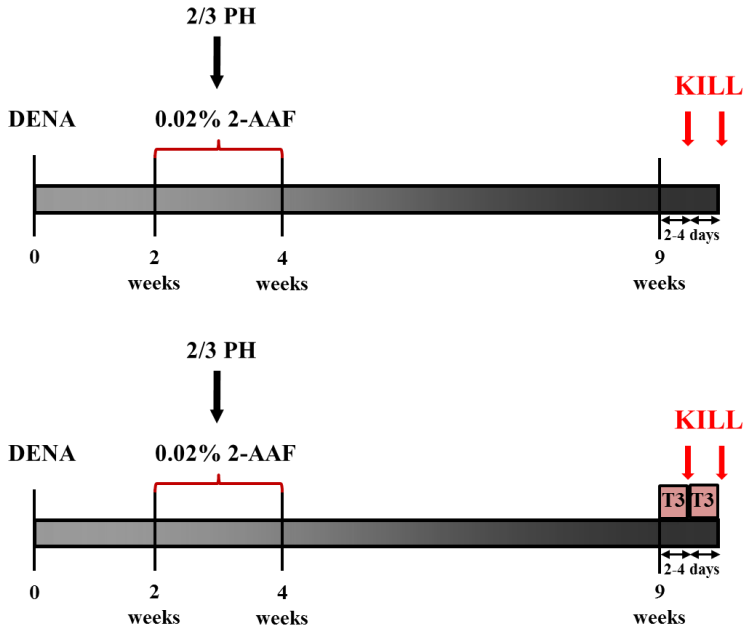

Figure 10 . Schematic representation of Experimental protocol 1.

Experimental protocol 2

Animals were subjected to R-H protocol as described in Experimental protocol 1. Following 2-AAF withdrawal, the animals were kept in basal diet till 10 months form DENA and then randomly divided into two groups: the first one was left on basal diet for another week, while the second group was exposed to a one-week treatment with T3 (4mg/kg of diet) (Figure 11).

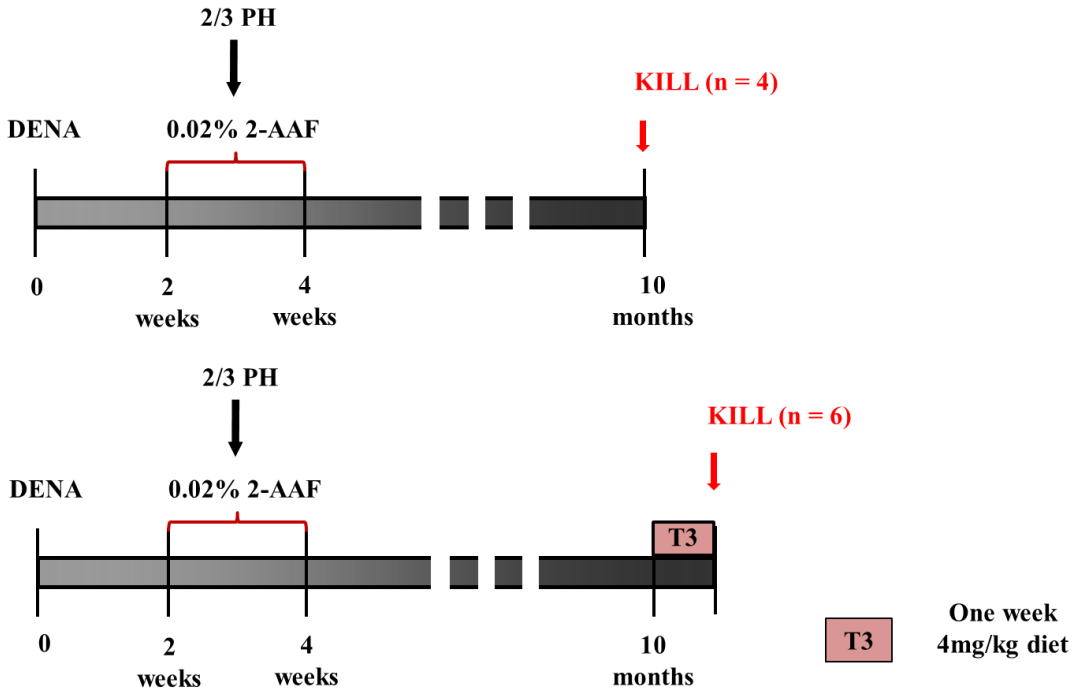

Figure 11 . Schematic representation of Experimental protocol 2.

Experimental protocol 3

Animals exposed to the R-H protocol and shifted to basal diet after 2-AAF withdrawal till 10 months from DENA were randomly divided into two groups: the first group was maintained in basal diet whereas the second group was exposed to 5 cycles of T3-diet (one-week cycle/every three weeks). All animals were sacrificed 14 months after treatment with DENA (Figure 12).

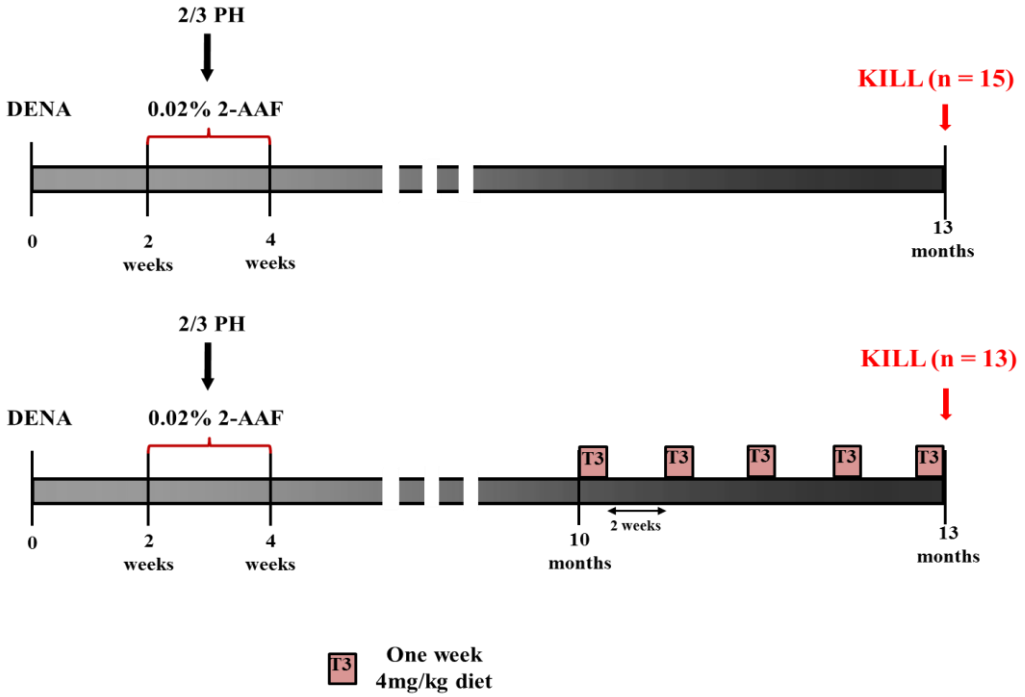

Figure 12 . Schematic representation of Experimental protocol 3.

Experimental protocol 4

Animals exposed to the R-H protocol and shifted to basal diet till 10 months from DENA were randomly divided into two groups: the first group was maintained in basal diet whereas the second group was exposed to 5 cycles of T3-diet (one-week cycle/every three weeks). Following the fifth cycle of T3, animals were fed a basal diet and killed 4 weeks thereafter (Figure 13).

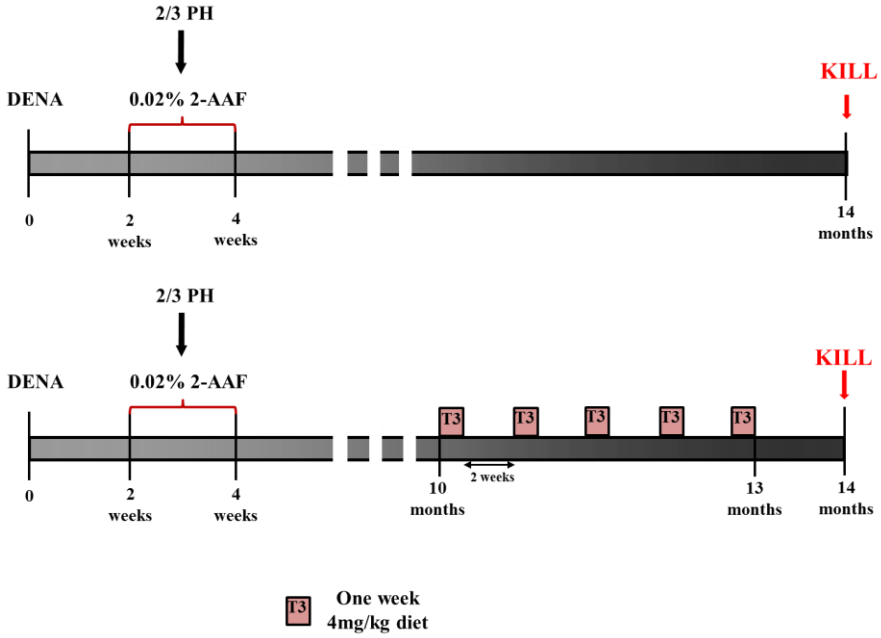

Figure 13 . Schematic representation of Experimental protocol 4.

Histology and immunohistochemistry

Tissue preservation

Immediately after the sacrifice, livers were cut in several pieces and preserved in different ways to carry out multiple analysis. For immunohistochemistry analysis, liver sections were fixed in 10% formalin, embedded in paraffin and stored at room temperature (RT). Other sections were immediately frozen in liquid nitrogen-cooled isopentane and preserved at -80°C for future molecular analysis and cryosectioning.

Hematoxylin and Eosin (H&E) staining

Four micron-thick paraffin-embedded liver sections were deparaffinised in Bioclear (Bio-Optica, Milan, Italy) for 30 minutes and hydrated in a decreasing series of alcohol. Sections were then incubated in Carazzi Hematoxylin for 22 minutes and after several washes in tap water, stained in 1% acidified alcoholic eosin for 14 seconds. Sections were then dehydrated through ascending alcohol series, cleared with Bioclear, air-dried and then mounted using synthetic mounting and coverslipped.

Glutathione S-transferase (GST-P) staining

4µm formalin-fixed sections were deparaffinised in Bioclear for 1 hour and hydrated in decreasing series of alcohol. Following two washes in phosphate buffered saline (PBS), the blocking of unspecific antibody binding sites was performed in 10% normal goat serum (Abcam, ab7481) for 30 minutes at RT. The next step was the overnight incubation with 1:1000 diluted rabbit anti-GSTP antibody (MBL, 311) at 4°C in humid chamber. To block endogenous peroxidase activity, slides were incubated in 0,5% hydrogen peroxide (Sigma-Aldrich) in distilled water for 10 minutes. Sections were then incubated with anti-rabbit Horseradish Peroxidase (HRP) secondary antibody (Sigma-Aldrich) at 1:300 dilution for 40 minutes at RT. Positive binding reaction was visualized using 3.3'-diaminobenzidine (DAB) (Sigma-Aldrich) for 6 minutes at RT. Afterwards, slides were counterstained with Harris Haematoxylin Solution (Bio-optica), dehydrated through graded alcohols, cleared and coverslips were mounted with synthetic mounting media.

KRT-19, MCT4, GLUT1, TIGAR, CS, NQO1, G6PD staining

4um-thick sections were deparaffinised in Bioclear for 1 hour and rehydrated in decreasing series of alcohol. Following two washes in PBS, antigen retrieval in Sodium Citrate Buffer was performed. Details regarding retrieval, primary and secondary antibody dilutions are described in Table 1.

Table 1. Details about retrieval, primary and secondary antibody dilutions used in the study.

Staining	Retrieval conditions	Primary antibody	Secondary antibody
KRT-19	2x6min MWO 700W	NBP1 78278 1:400 at 4°C ON incubation	Dako anti-rabbit, 60min RT
MCT4	4x5min MWO 700W	Rabbit sc50329, 1:50 at 4°C ON incubation	Dako anti-rabbit, 60min RT
GLUT1	NO	Rabbit ab652 1:400 at 4°C ON incubation	Dako anti-rabbit, 60min RT
NQO1	4x5min MWO 700W	Mouse ab28947 1:100 at 4°C ON incubation	Dako anti-mouse, 60min RT
TIGAR	5min MWO 700W	Rabbit AB10545 1:50 at 4°C ON incubation	Dako anti-rabbit, 60min RT
CS	NO	Rabbit ab96600 1:150 at 4°C ON incubation	Dako anti-rabbit, 60min RT
G6PD	NO	Sc67165 1:100 at 4°C ON incubation	Dako anti-rabbit, 60min RT

Complex II/Succinate Dehydrogenase (SDH) histochemical assay

Eight-micrometer-thick frozen sections were incubated at 37°C in incubation medium containing 0.2M phosphate buffer, sodium succinate solution, nitro blu tetrazolium (NBT) solution (Sigma-Aldrich) and distilled water. Successively, liver sections were rinsed in physiological saline, fixed in 10% formalin-saline solution, rinsed in 15% alcohol and finally mounted with an aqueous mounting medium. As succinate was oxidized to fumarate, the reduced form of NADH was produced and the reaction was visualized concomitantly with the electron acceptor reacting with the purple salt NBT.

Gamma glutamyl-transferase (GGT) histochemical assay

This assay was performed according to Rutenburg *et al*. [91]. Eight-micrometer-thick frozen sections were fixed in acetone at 4°C for 1 hour. Successively they were incubated for 15 minutes in a solution containing DMSO, NaOH, gamma glutamil-4metossi-2naftilamide, Glycylglycine, NaCl and fast blue. Sections were then washed in NaCl 0,85%, in $CuSO_4$, physiological solution and finally water. Slides were then mounted with glycerine.

Adenosine triphosphatase (ATPase) histochemical assay

As described by Wachstein e Meisel [92], 15um-thick frozen sections were incubated for 40 minutes at RT with a solution composed by ATP, $Pb(NO_3)_2$, $MgSO_4$ and distilled water. Slides were then washed in distilled water and successively in $(NH_4)_2S$. Finally, slides were mounted with glycerine.

Glucose-6-phosphatase (G6Pase) histochemical assay

15um-thick frozen sections were incubated for 40 minutes at RT with a solution composed by glucose-6-phosphate, $Pb(NO_3)_2$ and distilled water. Slides were then washed in distilled water and

successively fixed in 10% formalin for 30 minutes. Finally sections were washed in water and mounted with glycerine [93].

Enzymatic activity measurement on fresh tissue

For enzymatic activity measurement tissues frozen in liquid nitrogen-cooled isopentane and preserved at -80°C were cut with by cryostat in 16um-thick sections. For each sample 50 mg of liver tissue were prepared and preserved at -80°C before homogenizing in different buffers depending on the assay.

Respiratory chain complex I activity

The enzymatic activity of respiratory chain Complex I or NADH:ubiquinone oxidoreductase was assessed on liver lysates (5 μg of proteins per trace) previously homogenised in a buffer composed of 25 mM potassium phosphate pH 7.2, 5 mM $MgCl_2$, protease and phosphatase inhibitors. Samples were pre-incubated for 3 min at 37°C in a buffer composed of 25 mM potassium phosphate pH 7.4, 2 μM alamethicin, BSA 3 mg/ml, 500 μM sodium azide and 6.5 μM Coenzyme Q1. Reaction started after the addition of 30 μM NADH and the nucleotide reduction was recorded spectrophotometrically as a decrease in absorbance at 340 nm for 10 minutes. The Complex I activity was calculated as NADH consumption assessing the difference of the trace slopes with or without the Complex I inhibitor Rotenone and values were then normalised by protein amount.

Succinate dehydrogenase (SDH) activity

To measure the succinate-coenzyme Q reductase (SQR) enzymatic activity of respiratory chain complex II/succinate dehydrogenase (SDH), liver samples were homogenized in a buffer composed by 250mM sucrose, 10mM Tris-HCl, 0.1mM EGTA-Tris, pH 7.4, Percoll 10% protease and phosphatase inhibitors. Succinate-coenzyme Q reductase (SQR) enzymatic activity of SDH complex was assessed through spectrophotometric recordings following the reduction of 2,6-dichlorophenolindophenol (DCPIP) at 600nM. Samples (5 μg of proteins per trace) were pre-incubated for 10 minutes at 30°C in a buffer composed of 25mM potassium phosphate pH 7.2, 20mM sodium succinate and 5 μM alamethicin. After the pre-incubation time, sodium azide (5uM), antimycin A (2 μM), rotenone (2 μM) and DCPIP (50 μM) were added for 1 minute to the medium. Reaction was performed at 30°C and started after the addition of an intermediate electron acceptor (Coenzyme Q1, 65uM). Values were then normalized for protein amount.

Glucose-6-phosphate dehydrogenase (G6PD) activity

Liver samples were lysed at 4°C in a buffer composed of 140mM NaCl, 20mM Tris-HCl pH 7.4, 5mM EDTA, 10% glycerol, 1% Triton X-100, in the presence of phosphatase and protease inhibitors (Sigma). Lysates (10 μg) were then incubated with glucose-6-phosphate (1mM) and NADP+ (1.5mM). The rate of NADPH formation, which is proportional to the G6PD activity, was measured spectrophotometrically as an increase in absorbance at 340 nm at 30°C. Maleimide (12mM) was added as an inhibitor of 6-phosphogluconate dehydrogenase.

Laser capture microdissection

Sixteen-µm-thick serial frozen sections were cut and attached to 2-µm RNase-free PEN-membrane slides (Leica, Bannockburn, IL). To identify the localization of pre-neoplastic lesions, 6 µm thick sections were cut and stained for H&E, GST-P and KRT-19 to recognize positive lesions. Immediately before performing micro-dissection, frozen sections were rapidly stained with a 3.5 minutes H&E procedure. Briefly, sections were hydrated (30 seconds in Ethanol 100% and 95%), stained in Mayer's hematoxylin for 90 seconds, washed in water for 20 seconds, stained in 0.25% alcoholic Eosin for 10 seconds and dehydrated by Ethanol 100% for 30 seconds. Micro-dissection was performed using a Leica laser microdissection apparatus (LMD6000). The whole procedure was performed within 20 minutes to avoid RNA degradation. To guarantee the maximum amount of material, the same lesion was identified and cut from 5 to 10 serial sections. Dissected material from the same nodule was collected in the same o.5ml micro centrifuge tube's cup filled with 50µl of Lysis/Binding Buffer. At the end of the procedure, microtubes were plugged up, span to collect dissected material and immediately frozen at -80°C until extraction with mirVana miRNA Isolation Kit (Ambion, AM1560).

RNA extraction

RNA extraction from pre-neoplastic lesions

mirVana miRNA Isolation Kit (mirVana, Ambion, Life Technologies, Monza) was used for the extraction of total RNA from pre-neoplastic lesions and from the corresponding control livers. Briefly, once microdissected, collected lesions were dissolved in 300µl of Lysis Buffer (LB) and 30µl of miRNA Homogenate Additive. After a 10 minutes incubation on ice, organic extraction of RNA was performed adding 300µl of acidphenol:chloroform:isoamyl alcohol (125:24:1) to each sample. Successively samples were centrifuged for 5 minutes at maximum speed in order to separate the aqueous and organic phases. After recovery of the RNA-containing aqueous phase, 1.25 volumes of 100% ethanol were added, and the mixture was transferred to a filter cartridge. Collecting tubes were centrifuged and the flow-through was discarded. Following three washing steps with Wash Buffers, filters were dried by 60 seconds full speed centrifugation. Finally, RNA was eluted with pre-heated (95°C) RNAse-Free distilled water and stored at -80°C.

RNA extraction from rat HCCs and control livers

Sixteen µm-thick frozen sections were cut from different lobes of each liver. The sections were collected in 0.5ml tubes and stored at -80°C until extraction. Total RNA extraction was then performed using TRIzol Reagent (Invitrogen). Briefly, tissue samples were homogenized with 800µl of TRIzol Reagent and centrifuged for 10 minutes at 12000rpm. After adding to the supernatant 800µl of chlorofom and shaking vigorously, a further centrifugation allowed to separate the RNA-containing aqueous phase. RNA was then precipitated by mixing the aqueous phase with isopropyl alcohol. After centrifugation, the RNA pellet was washed once with 75% ethanol and then dissolved in RNAse-free distilled water before storing at -80°C.

Quantitative and quality analysis of nucleic acids

Total RNA concentrations and purity ratios (260/280 and 260/230) were measured using NanoDrop 1000 Spectrophotometer (Thermo Scientific, France). RNA integrity was evaluated by Agilent Bioanalyzer 2100 (Agilent Technologies) by assessing the RNA Integrity Number (RIN). Only RNA samples with a RIN equal to or higher than 7 were further used in the study. All procedures were performed according to manufacturer's protocol.

Microarray

The RatRef-12 V1 Beadchip Illumina, containing 21791 gene-specific oligonucleotides, was used to perform gene expression profile analysis. Four Chips were loaded to investigate 48 samples divided in the following groups:

- 8 samples were obtained by micro-dissection of untreated rat liver tissue as matched-age absolute controls;
- 10 samples consisted in a pool of KRT-19 positive pre-neoplastic lesions microdissected from rats subjected to the R-H protocol and sacrificed at 2 and 4 days after 9 weeks from DENA initiation;
- 10 samples were obtained by micro-dissecting a pool of KRT-19 positive pre-neoplastic nodules from rats subjected to the R-H protocol and fed a T3 diet for 2 days;
- 10 samples were obtained by micro-dissecting a pool of KRT-19 positive pre-neoplastic nodules from rats subjected to the R-H protocol and fed a T3 diet for 4 days;
- 10 samples were collected by micro-dissecting a pool of KRT-19 negative pre-neoplastic lesions from rats subjected to R-H protocol.

RNA amplification

Illumina TotalPrep RNA amplification kit (Ambion, Life Technologies, Milano) was used to perform amplification of 150ng of total RNA. With this procedure is possible to generate biotinylated, amplified RNA for hybridization with Illumina Sentrix arrays. The protocol consists of a reverse transcription with an oligo primer bearing a T7 promoter using a reverse transcriptase to produce higher yields of first single-strand cDNA. Successively, cDNA goes through a second strand synthesis and it is cleanup to become a template for in vitro transcription (IVT) with T7 RNA Polymerase. During this step biotin-UTPs are used to generate a great amount of biotinylated, antisense RNA copies (cRNA). The labelled cRNA produced with this procedure are then used for the hybridization with Illumina arrays.

BeadChips Illumina hybridization

A total of 750 ng biotinylated cRNA were hybridized for 18hrs to RatRef-12 V1 BeadChip. Hybridized chips were washed and stained with streptavidin-conjugated Cy3 (GE Healthcare Milano, Italy). BeadChips were dried and scanned with an Illumina BeadArray Reader (Illumina Inc., San Diego, CA, USA).

Microarrays data analysis

For data analysis, the intensity files were loaded first into the BeadStudio 3.0.14 Software (Illumina Inc., San Diego, CA, USA) to extract the fluorescence values and for quality control analysis. The extracted values were then loaded BRB Array Tools (Version 4.4.0) for gene expression analysis. First, the quantile normalization algorithm was applied on the dataset to correct systematic errors. This method normalizes a matrix of probe level intensities using a normalization based upon quantiles.

Only genes whose expression differed by at least 1.5-fold from the median in at least 20% of the arrays and characterized by a 50^{th} percentile of intensities greater than 300 were considered as detected. According to these criteria, 869 expressed transcripts out of 21.791 showed reproducible up- or down-regulation. Hierarchical cluster analysis (Heat-Map) divided the experimental groups in different clusters depending on their grade of expression profile similarity. Data were organized as a tree diagram called dendrogram in which the distance between the branches represented the dissimilarity among the groups. In this map, green color indicates a low fluorescence intensity, representing down-regulated elements whereas red color indicates a high fluorescence intensity representing up-regulated elements.

F-test (with random variance model) and multivariate permutation test (Confidence level of false discovery rate assessment: 80%, Maximum allowed proportion of false-positive genes: 0.1) were used to identify genes differentially expressed. Following this analysis, 864 genes were differently expressed. Among these genes, 17 genes belonging to metabolic pathways were selected to create the Heat-Map reported in Results.

IPA (Ingenuity Pathway Analysis)

Genes were classified according to their role in biological process, cellular components, and molecular function using Ingenuity Pathway Analysis (IPA), a web-based functional analysis tool developed by Ingenuity Sistems (www-ingenuity.com). IPA is a powerful resource to identify the most relevant signalling pathways, molecular networks and biological functions for genes of interest. Moreover, it can predict the activation and inhibition of upstream transcription factors and the direction of downstream effects on biological and disease processes. Pathway analysis was carried out on genes found to be significantly modified (cut off up-regulated>+2 and down-regulated<-2). Afterwards, genes were correlated to specific biological functions and it was possible to identify transcription factors implicated in the expression of the genes present in our dataset.

Analysis of mRNA expression levels

Reverse Transcription Polymerase Chain Reaction (RT-PCR)

To investigate by quantitative real time-PCR (qRT-PCR) mRNA expression levels of *Dio1, Spot14, Gst-p, Krt-19, Glut1, Hk2, G6pd, Taldo1, Tkt,* and *Nqo1,* total RNA was retro-transcribed to cDNA using the High Capacity cDNA Reverse Transcription Kit (Applied Biosystem, Life Technologies, Italy).

The reaction mixture contained: 2µl of RT buffer (10X), 2µl of Random Primers (10X), 0.8µl of dNTP mix (100mM), 1µl of MultiScribe Reverse Transcriptase, 1µl of DNase/RNase-free distilled water and 10µl of the appropriate total RNA at the desired concentration. Thermo cycle condition was: 25°C for 10 minutes, 37°C for 120 minutes and 85°C for 5 minutes, followed by a 4°C hold. Samples were then stored at -20°C until next use.

Quantitative real-time PCR (QRT-PCR)

Once retro-transcribed, cDNAs were used for the assessment of mRNA gene expression analysis performed by qRT-PCR. The amplification reaction was performed in a final volume of 10µl mixture containing: 4µl of cDNA template (2ng/µl), 5µl of 2X TaqMan Gene Expression Master Mix (Applied Biosystem, Life Technologies, Italy), 0.5µl of 20X TaqMan assay (Applied Biosystem, Life technologies, Italy) and 0.5µl of RNase-free water.

The following TaqMan probes were used:

- Rn00572183_m1 for the analysis of rat *Dio1;*
- Rn01511034_m1 for the analysis of rat *Spot14;*
- Rn00561378_gH for the analysis of rat *Gst-p;*
- Rn1496867_m1 for the analysis of rat *Krt-19;*
- Rn01417099_m1 for the analysis of rat *Slc2a1/Glut1*;
- Rn00562457_m1 for the analysis of rat *Hk2;*
- Rn01529640_g1 for the analysis of rat *G6pd*;
- Rn00582620_m1 for the analysis of rat *Taldo1;*
- Rn01453456_g1 for the analysis of rat *Tkt;*
- Rn00566528_m1 for the analysis of rat *Nqo1;*
- Rn00578115_m1 for the analysis of rat *Slc16a3/Mct4.*

Reactions were performed in ABI PRISM 7300HT thermocycler Applied Biosystem, Life Technologies, Italy); the cycle conditions were set as follows: 50°C for 2 minutes and 95°C for 10 minutes, followed by 40 cycles at 95°C for 15 seconds and at 60°C for 1 minute. Each sample was analysed in triplicate; the housekeeping gene rat *Gapdh* (glyceraldehyde-3 phosphate dehydrogenase) was used for normalization. To determine the relative expression levels of each gene the 2-ΔΔCT method was used. The threshold cycle (Ct) value of the target gene was normalized to that of the endogenous reference and compare with a calibrator.

Statistical analysis

Data are expressed as mean ± standard error (SEM). Analysis of significance was done by t Student's test and by One Way ANOVA using the GraphPad software (La Jolla, California).

Summary of experimental protocols

Experimental protocols and relative scientific questions, experimental design and methods are summarized in the following table 2.

Table 2.

Experimental protocol	Scientific questions	Experimental design	Methods and biomarkers investigated
1	• Is the observed T3-dependent regression of pre-neoplastic lesions associated to the ability of T3 to interfere with their metabolic reprogramming?	R-H protocol + 4 days T3-supplemented diet starting 9 weeks after DENA	• Transcriptomic analysis of laser-microdissected nodules • IHC of GST-P, KRT-19, G6PD, SDH activity
2	• Do fully developed HCCs retain the ability to respond to T3 administration? • Is a brief T3 treatment able to impact on the metabolic reprogramming of neoplastic hepatocytes?	R-H protocol + 7 days T3-supplemented diet starting 10 months after DENA	• RT-PCR and IHC of *Dio1, Gst-p, Krt-19, Glut1, Hk2, Taldo1, Tkt, G6pd*, CS, TIGAR, MCT4, *Nqo1* • Complex 1, complex 2 and G6PD activity
3	• Are repeated cycles of T3 able to inhibit tumor growth and revert the metabolic reprogramming of cancer cells?	R-H protocol + 5 cycles T3-supplemented diet starting 10 months after DENA	• RT-PCR and IHC of *Dio1, Spot14 Gst-p, Krt-19, Glut1, Hk2, Taldo1, Tkt, G6pd*, CS, TIGAR, MCT4, *Nqo1* • Complex 1, complex 2 and G6PD activity
4	• Is the effect of T3 maintained after hormone withdrawal?	Experimental protocol 3 followed by 1 month on basal diet	• *Dio1, Spot14, Krt-19, Nqo1, G6pd*

RESULTS AND DISCUSSION

T3 administration induces a switch of the metabolic profile of KRT-19+ pre-neoplastic nodules.

Previous studies from our laboratory showed that metabolic reprogramming takes place at early stages of rat hepatocarcinogenesis [62]. Interestingly, only those pre-neoplastic lesions that are positive for the progenitor/stem cell marker KRT-19 exhibit a Warburg profile [62]. In the RH protocol while only 25% of the GSTP+ pre-neoplastic lesions show positivity for this marker, almost all the fully developed HCCs are KRT-19+ [67]. Moreover, a similar gene expression profile between KRT-19+ nodules and HCCs has been observed, indicating KRT-19+ pre-neoplastic lesions as the precursor cell population for HCCs [68]. In this context, metabolic reprogramming may represent a hallmark of more aggressive lesions, providing a growth selective advantage to KRT-19+ hepatocytes.

KRT-19+ pre-neoplastic lesions, similarly to what observed in HCCs, are characterized by deregulation of the T3/TR axis leading to a local hypothyroid status [80]. Accordingly, treatment of nodule-bearing rats with T3 for 7 days causes a 70% reduction of GSTP+ pre-neoplastic lesions, compared to the untreated group [90]. Nodule regression involved both KRT-19- and KRT-19+ lesions, but preferentially the latter type, ranging from 27% of total lesions to 9% 7 days after T3 treatment [80]. Taken together, these data prompted us to further investigate whether the regression of pre-neoplastic lesions caused by T3 could be due to the ability of T3 to interfere with their metabolic reprogramming.

To investigate the effect of T3 on pre-neoplastic lesions, 10 weeks after DENA administration rats were fed a T3-supplemented diet for 2 and 4 days, times preceding T3-induced nodule regression. After sacrifice, we isolated KRT-19+ and KRT-19- pre-neoplastic nodules by laser-microdissection and performed a transcriptomic analysis using the Illumina platform. We focused our attention on genes involved in glucose metabolism. As shown by the Heatmap in Figure 14A, unsupervised analysis separated KRT-19+ from KRT-19- nodules. Interestingly, KRT-19- nodules co-clustered with control samples. A 2-day T3 treatment was able to modify the expression of some metabolic genes. This effect was even more evident after 4-day treatment. Indeed, the expression profile of KRT-19+ lesions treated with T3 no longer co-clustered with KRT-19+ nodules, but rather with KRT-19- and controls. Among the changes induced by T3, the most marked affected the Pentose Phosphate Pathway (PPP). Indeed, either *G6pd*, the limiting enzyme of the oxidative branch of PPP, as well as *Taldo1* and Phosphogluconate dehydrogenase (*Pgd*), involved in the non-oxidative and oxidative PPP respectively, were up-regulated in KRT-19+ pre-neoplastic nodules when compared to KRT-19- lesion or to controls. Overall these results show that T3 induces a reversion of Warburg metabolism towards a differentiated hepatocytes' metabolic profile. (Figure 14A). Accordingly, functional comparison of KRT-19+ pre-neoplastic nodules and KRT-19+ nodules treated with T3 for 4 days, revealed among the most enriched pathways, those related to metabolism (Figure 14B).

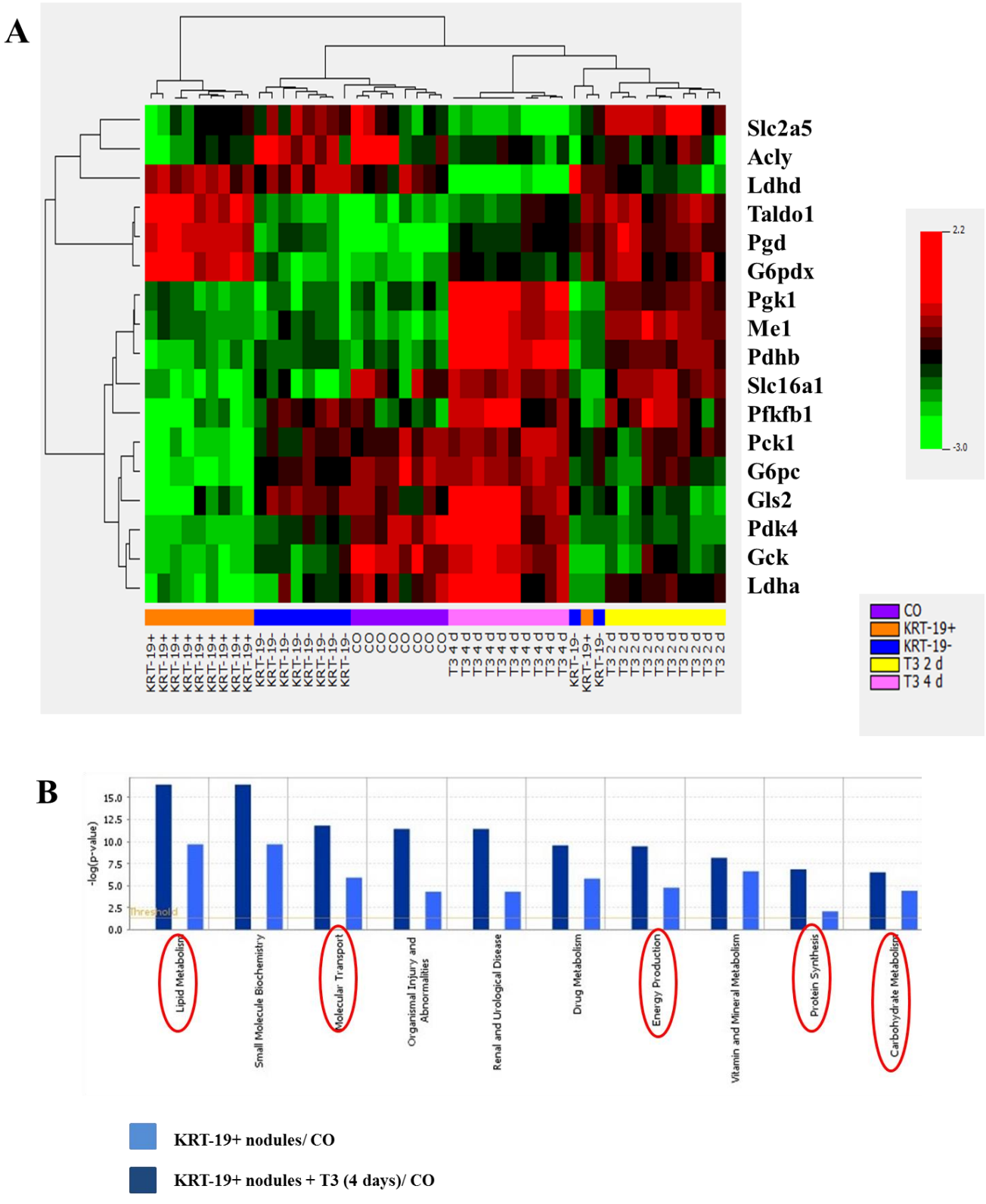

Figure 14 . (A): Unsupervised hierarchical clustering of metabolic gene expression profile in KRT-19+ nodules after 2 days T3-treatment (KRT-19+ T3 2d), age-matched controls (CO), KRT-19- and KRT-19+ nodules after 4 days T3-treatment (KRT-19+T3 4d). Red and green colours represent higher or lower expression levels of the genes, respectively. **(B):** Functional analysis of differentially expressed genes in KRT-19+ pre-neoplastic nodules treated or not with T3 for 4 days. Top 10 enriched functions. P values were determined using Ingenuity scoring system and were judged significant at $P < 0.05$.

To further investigate at a protein level the effect of T3 on metabolism, we performed immuno- and histochemical analysis on serial sections from liver of nodule-bearing rats treated or not with T3 for 4 days. Nodules were firstly identified by their positivity to the neoplastic marker GST-P (Figure 15 A, E, I, N, Q, S). These nodules exhibited increased activity of gamma glutamyl transpeptidase (GGT) and decreased activity of adenosine triphosphatase (ATPase), while they were not expressed or highly expressed in the surrounding normal tissue, respectively (Figure 15 B and D). Interestingly, treatment with T3 reduced the activity of GGT, while concomitantly inducing that of ATPase in pre-neoplastic nodules (Figure 15 F and H). These data support the hypothesis that the need for ATP of cancer cells is not as critical as the need for carbons and NADPH [10]. Moreover, the activity of Glucose-6-phosphatase (G6Pase), whose deficiency is associated to HCC development, was impaired in pre-neoplastic nodules and rescued by T3, as shown by histochemical analysis [94] (Figure 15 C and G). These data led us to hypothesize that T3 treatment of nodule-bearing rats may induce a switch to a more differentiated phenotype.

To further investigate the capability of T3 to interfere with metabolic reprogramming of pre-neoplastic lesions, we analysed the expression of Glucose-6-Phosphate Dehydrogenase (G6PD), the rate-limiting enzyme of the PPP, whose expression and activity have been shown to increase in KRT-19+ pre-neoplastic nodules and HCC [62]. As shown in Figure 15 (M and P), while we confirmed an increased protein content of G6PD in KRT-19+ nodules, the expression of G6PD was completely abolished after T3 treatment, indicating a decreased activation of the pathway.

Along with enhanced glycolysis and diversion of metabolites to biosynthetic pathways, mitochondrial respiration is usually impaired in pre- and neoplastic lesions [62]. An indicator of mitochondrial functionality is Succinate Dehydrogenase (SDH) which not only takes part to the TCA cycle, but it is also the complex II of the respiratory chain. When we analysed the activity of SDH, we found that while its activity was totally impaired in pre-neoplastic nodules, it was restored after treatment with T3 (Figure 15 R and T). These results suggest that a short T3 treatment of pre-neoplastic nodules may induce a return to a normal metabolic profile by switching metabolism from glycolysis to OXPHOS. Since, these changes are observed between 2 and 4 days after the beginning of T3 treatment and precede the disappearance of the nodules, it is possible to hypothesize that this metabolic rewiring could be one of the mechanisms responsible for the regression of the nodules observed after 7 days of treatment.

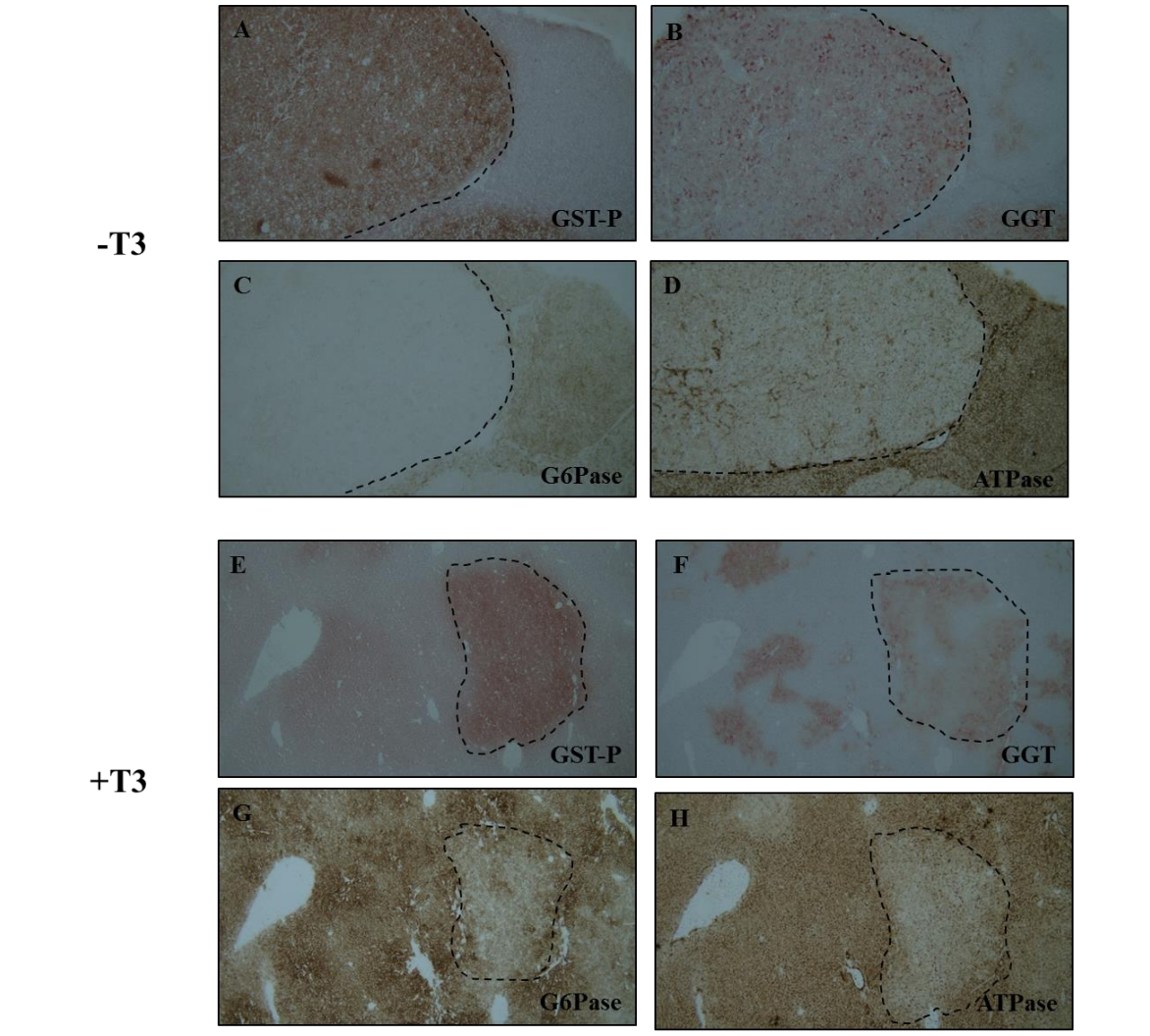
-T3
A
GST-P
B
GGT
C
G6Pase
D
ATPase
+T3
E
GST-P
F
GGT
G
G6Pase
H
ATPase
-T3
I
GST-P
L
KRT-19
M
G6PD
+T3
4days
N
GST-P
O
KRT-19
P
G6PD

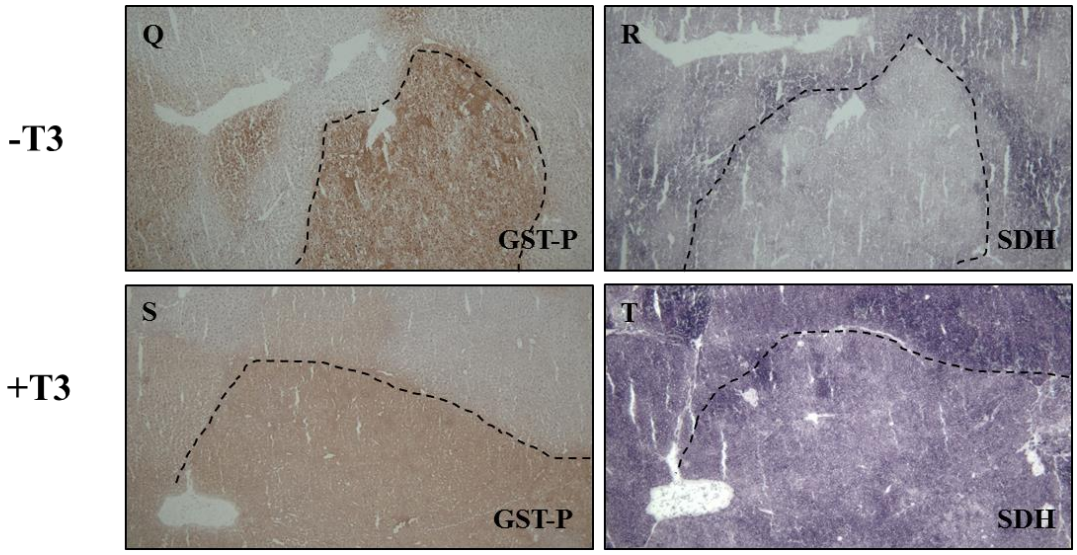

Figure 15 . Immuno- and histochemical analysis of serial sections of livers from nodule-bearing rats treated or not with T3 for 4 days (magnification 5x).

HCCs are still responsive to T3

Unfortunately, HCC in the majority of patients is usually diagnosed at advanced stage of disease. Since at this stage no effective therapeutic strategies are available, novel strategies for the cure of this lethal cancer are urgently needed.

Based on this premises, we investigated whether the anti-tumoral effect of T3 observed on pre-neoplastic lesions could also affect established HCCs. Since cancer cells are known to be resistant to uptake and biotransformation of most drugs, we performed initial experiment to determine whether HCC could still respond to T3.

To this aim, rats exposed to the RH protocol were sacrificed 10 months after DENA initiation, while another group of rats was fed a T3 supplemented diet for one week starting from the same time point. A group of absolute controls, not exposed to the RH protocol, was also included.

Histological analysis of samples from rats not treated with T3, revealed the presence of several cellular alterations, ranging from dysplastic nodules, either low grade (LGDN) as well as high grade (HGDN), to fully developed HCCs. LGDN were characterized by well differentiated hepatocytes arranged in up to 4 cells thick trabeculae. Most of them showed regular edges and a circular shape. In HGDN hepatocytes were arranged in more thick layers and showed increased nuclear/cytoplasmic ratio, increased number of apoptotic cells and mitotic figures. Few cells showed prominent nucleoli. HCCs showed a clear alteration of architecture, ranging from the classical trabecular pattern to a undifferentiated solid pattern. Some HCCs showed also a significant intratumoral variability, with mixed patterns. One week of T3 diet feeding resulted in the improvement of microscopic architecture, with reduced thickness of the trabeculae. Moreover, most lesions showed areas of regression, indicated by the presence of differentiated hepatocytes, arranged in normal trabecular pattern, within the neoplastic area (Figure 16)

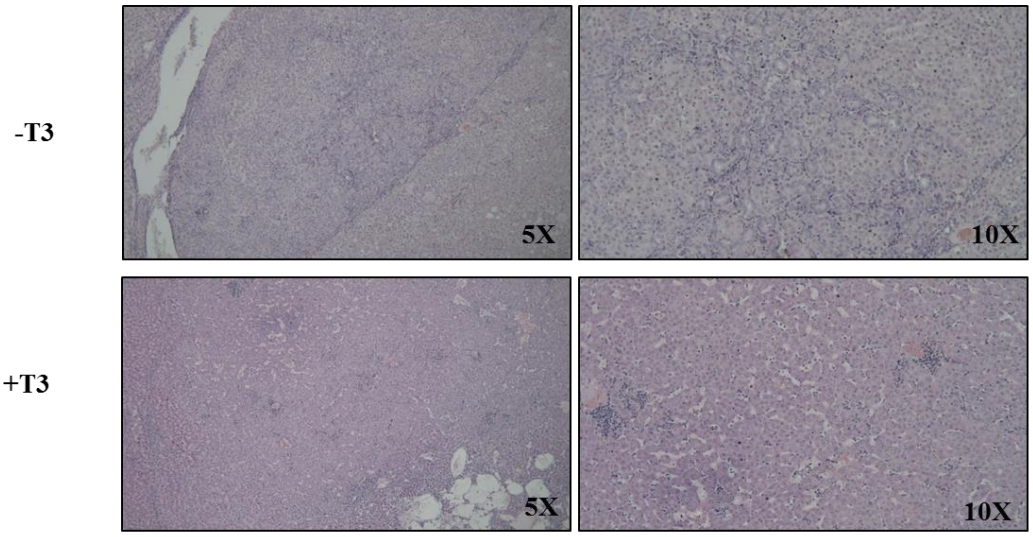

Figure 16 . Histological observation of the tumors by Hematoxylin and Eosin (H&E) staining under light-field microscope with 5x and 10x magnification.

Since dysregulation of T3/TR axis characterizes HCCs, to investigate whether these tumors are still responsive to T3, we performed gene expression analyses of classical THRβ target genes, namely Deiodinase 1 (*Dio1*), the deiodinase isoform typically expressed in the liver, and *Spot14*, in the three experimental groups [80,95]. As expected, *Dio1* and *Spot14* mRNA levels were significantly down-regulated in HCCs compared to untreated controls. Treatment with T3 was able to restore *Dio1* as well as *Spot14* mRNA levels although the difference in the expression of the latter gene was not statistically significant. (Figure 17 A). In addition, gene expression analyses showed a strong up-regulation of the neoplastic marker *Gst-p* and the progenitor marker *Krt-19* in the liver of HCCs bearing rats compared to the absolute controls. As expected, a significant decrease of *Gst-p* and *Krt-19* expression was also achieved by treatment with T3 (Figure 17 B and C). Finally, IHC revealed a strong reduction of GST-P and KRT-19 staining in the tumors after T3 treatment (Figure 22 A and B). Taken together, these results clearly show that HCCs are still able to respond to T3.

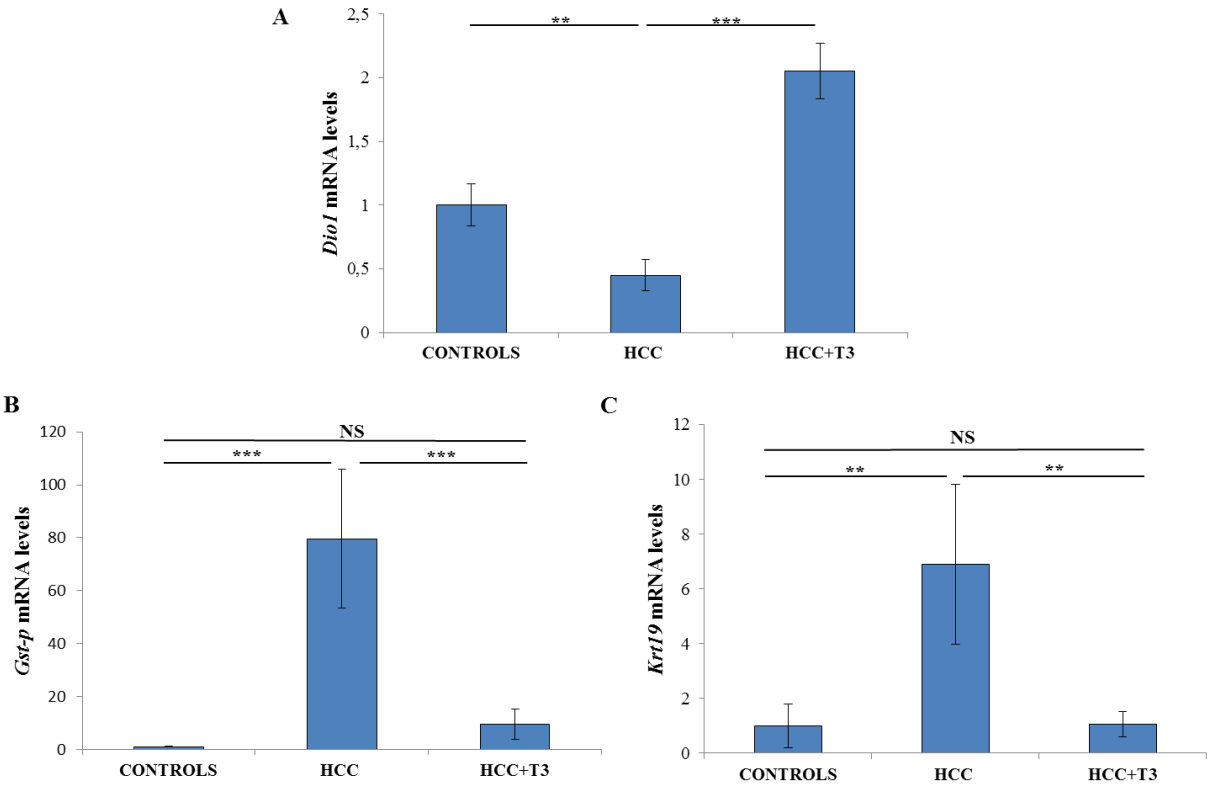

Figure 17 . mRNA expression of *Dio1*, *Gst-p* and *Krt-19* was assessed by qRT-PCR in controls, HCCs and HCCs+T3. Gene levels were calculated as fold change and normalized using rat *Gapdh* as endogenous control. ***P < 0.001; **P < 0.01; NS: not significant.

T3 administration induces a reversion of the metabolic profile of HCCs

To assess whether treatment with T3 could induce a reversion in the metabolic profile of cancer cells, we performed several analyses on mRNA levels and content of proteins with key roles in glycolysis, PPP and OXPHOS.

According to the Warburg effect, cancer cells relying on glycolysis, up-regulate glucose transporters (GLUT1) and the first enzyme of the glycolytic pathway Hexokinase 2 (HK2), in order to increase the import of glucose molecules in the cytoplasm and prevent their efflux back into the extracellular space [40]. Regarding HCC, increased expression of GLUT1 and HK2 have already been reported [96,97]. The results showed that both mRNA and protein levels of *Glut1* were decreased after T3 treatment. Moreover, administration of the hormone caused a strong inhibition of the *Hk2* mRNA levels in the T3 treated group, compared to the untreated HCCs (Figure 18 A and B; Figure 21; Figure 22).

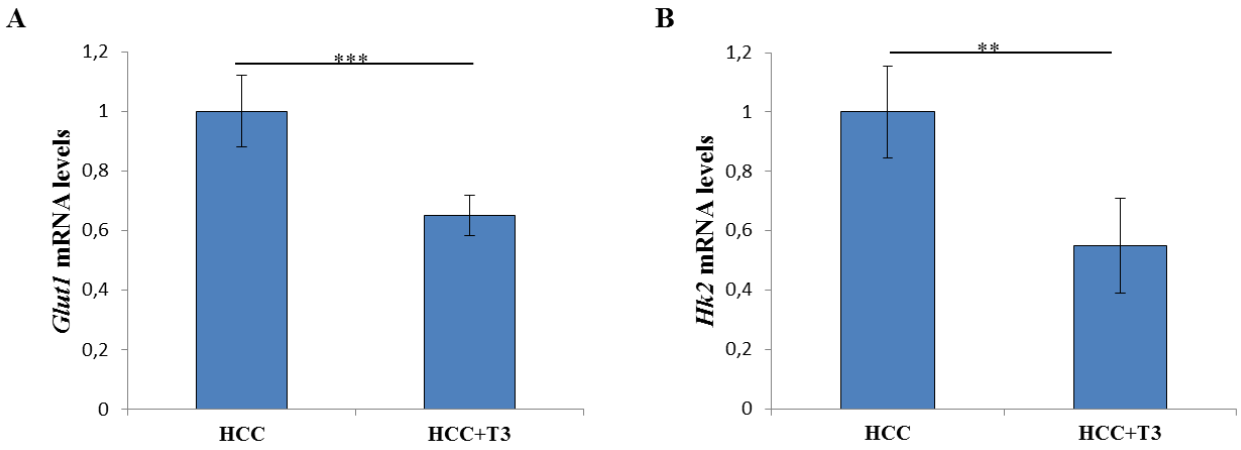

Figure 18 . mRNA expression of *Glut1* (A) and *Hk2* (B) was assessed by qRT-PCR in HCCs and HCCs+T3. Gene levels were calculated as fold change and normalized using rat *Gapdh* as endogenous control. ***P < 0.001; **P < 0.01.

In cancer cells a number of intermediate glucose metabolites is redirected into the PPP in order to supply the need of ribose-5-phosphate and NADPH to support proliferation and help maintain cellular redox capacity, respectively [2]. A direct consequence of this alteration is an up-regulation of enzymes involved in PPP, frequently found in HCC. For this reason, we examined the expression of genes encoding enzymes involved in the oxidative and non-oxidative branch of the PPP. As demonstrated by gene expression analysis, Transaldolase1 (*Taldo1*) and Transketolase (*Tkt*) mRNA levels, both enzymes of non-oxidative branch of the PPP, were down-regulated after T3 treatment (Figure 19 A and B). In addition, *G6pd* was significantly up-regulated both at mRNA (Figure 19 C) and protein levels (Figure 21 and Figure 22) in the HCCs compared to the controls while a massive down-regulation took place after T3 treatment. T3 also strongly inhibited the activity of G6PD, an enzyme strongly induced in HCCs not exposed to the hormone (Figure 19 D).

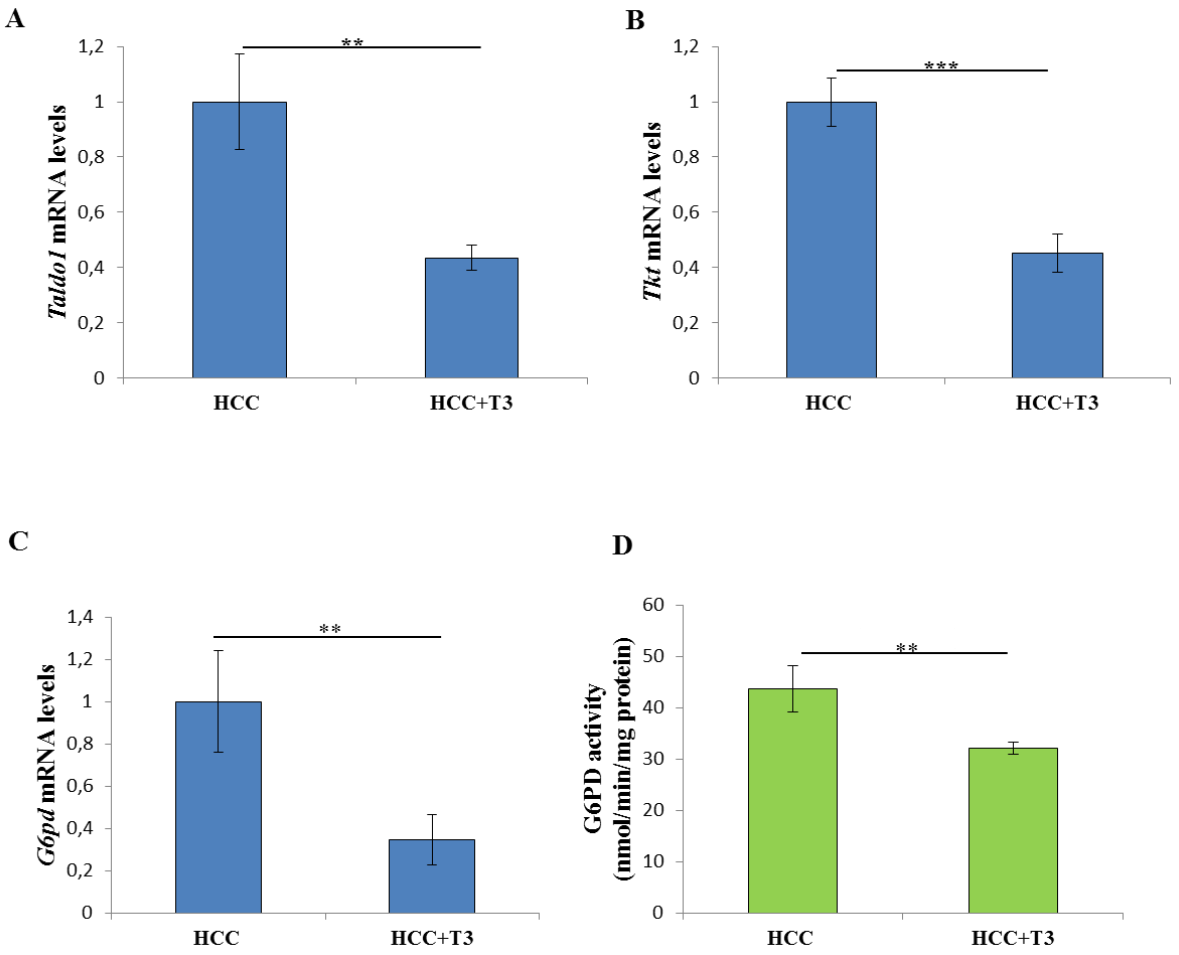

Figure 19 . mRNA expression of *Taldo1* **(A),** *Tkt* **(B)** and *G6pd* **(C)** was assessed by qRT-PCR in HCCs and HCCs+T3. Gene levels were calculated as fold change and normalized using rat *Gapdh* as endogenous control. ***P < 0.001; **P < 0.01. **(D)** G6PD activity was measured in HCC and HCC+T3. **P < 0.01.

Diversion of glucose metabolites to PPP is often favoured by induction of the fructose-2,6-bisphosphatase TIGAR that leads to inhibition of phosphofructokinase 1 (PFK1), thus reducing the glycolytic flux downstream this step [35]. Accordingly, while TIGAR was found increased in HCC compared to the surrounding tissue, its expression almost completely disappeared after T3 treatment (Figure 21 and Figure 22).

PPP activation has recently been proposed as one of the mechanisms by which deregulated NRF2/KEAP1 pathway contributes to cellular proliferation and tumorigenesis, being *G6pd*, *Tkt* and *Taldo1* target genes of NRF2 [98]. Previous results from our laboratory showed the ability of T3 to inhibit the NRF2-dependent pathway in pre-neoplastic nodules [99]. In line with these observations, we found a strong activation of the NRF2 pathway in HCC, as showed by protein and mRNA levels of NAD(P)H:quinone oxidoreductase 1 (*Nqo1*), a well-known NRF2 target gene. As previously observed in pre-neoplastic lesions, *Nqo1* levels decreased after T3 treatment also in HCC, both at mRNA and protein levels (Figure 20; Figure 21; Figure 22).

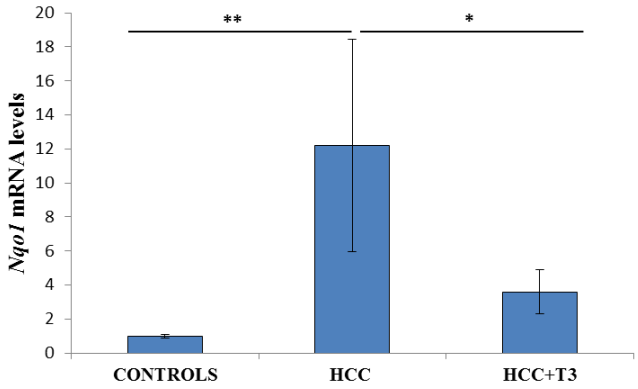

Figure 20 . mRNA expression of *Nqo1* was assessed by qRT-PCR in controls, HCCs and HCCs+T3. Gene levels were calculated as fold change and normalized using rat *Gapdh* as endogenous control. **P < 0.01; *P < 0.05.

Most tumor cells convert any excess of glycolytic flux not utilized for biosynthesis in lactate that is subsequently excreted out of the cell through monocarboxylate transporters (MCTs) [2]. In general, tumor tissues up-regulate MCTs because of their need to maintain an intracellular acid-base balance [100]. Among all the MCTs isoforms, MCT4 has recently been correlated with poor prognosis in hepatocellular carcinoma [101]. When we analysed protein levels of MCT4, we found an increased content in HCC compared to the surrounding tissue. Conversely, an obvious decrease was evident in the tumors after T3 treatment (Figure 21; Figure 22).

Similarly, IHC of serial sections showed an increased expression of citrate synthase (CS) in the tumors and a decrease after T3 treatment (Figure 21; Figure 22). Since in rat HCCs glycolysis seems to be down-regulated downstream of PFK1 reaction, increased CS expression could be explained considering that cancer cells often increase the uptake of acetate that can be used to fuel the TCA cycle. Acetate is converted into acetyl-CoA which, in turn, may fuel the TCA cycle, leading to citrate production through CS. Moreover, once produced, citrate can participate in down-regulating glycolysis, being an allosteric inhibitor of PFK1 [40].

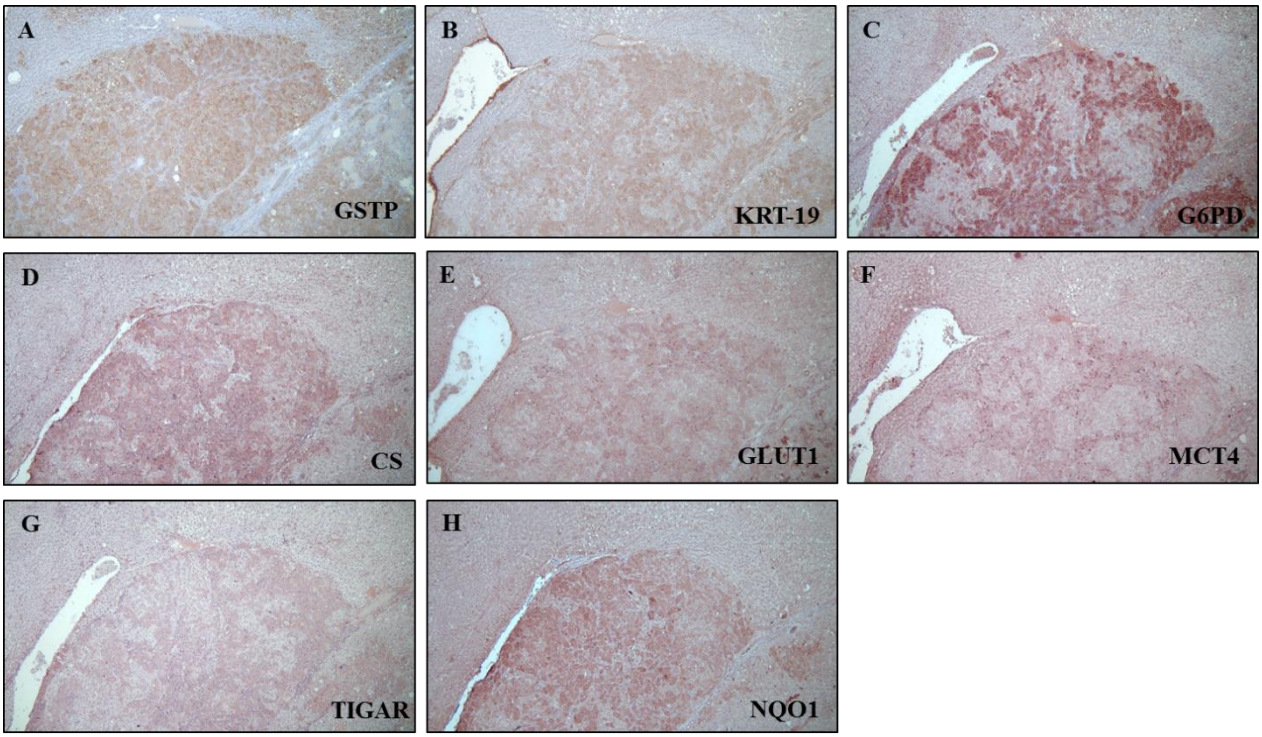

Figure 21 . Immunohistochemical analysis of serial paraffin sections from livers of HCC bearing rats showing a perfect match between G6PD, CS, GLUT1, MCT4, TIGAR, NQO1 and GST-P and KRT-19 positivity (5x).

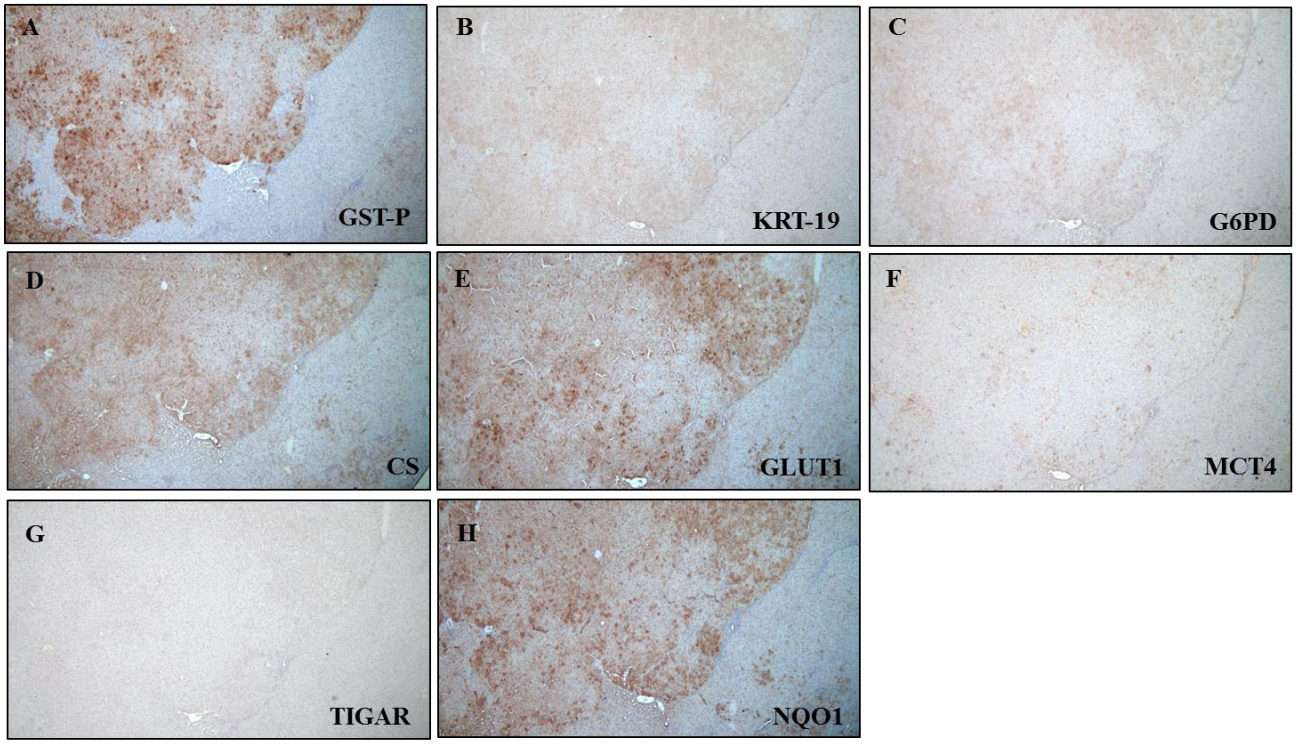

Figure 22 . Immunohistochemical analysis of serial paraffin sections from livers of HCC bearing rats treated with T3 for 7 days showing a loss of KRT-19, G6PD; MCT4 and TIGAR positivity and a decreased positivity for GST-P, CS, GLUT1 and NQO1. (5x).

Along with up-regulation of glycolysis and PPP, a decrease in mitochondrial respiration is often observed in some tumors. Thus we wondered whether T3 dependent metabolic restoration involved also mitochondrial respiration.

To this aim, we analysed the activity of both complex I and complex II (SDH) of the respiratory chain, both of them providing electrons for the complex III. We found that while the activity of both the complexes was inhibited in HCC, T3 treatment rescued their activity, suggesting a T3-dependent reactivation of the mitochondrial respiration. (Figure 23).

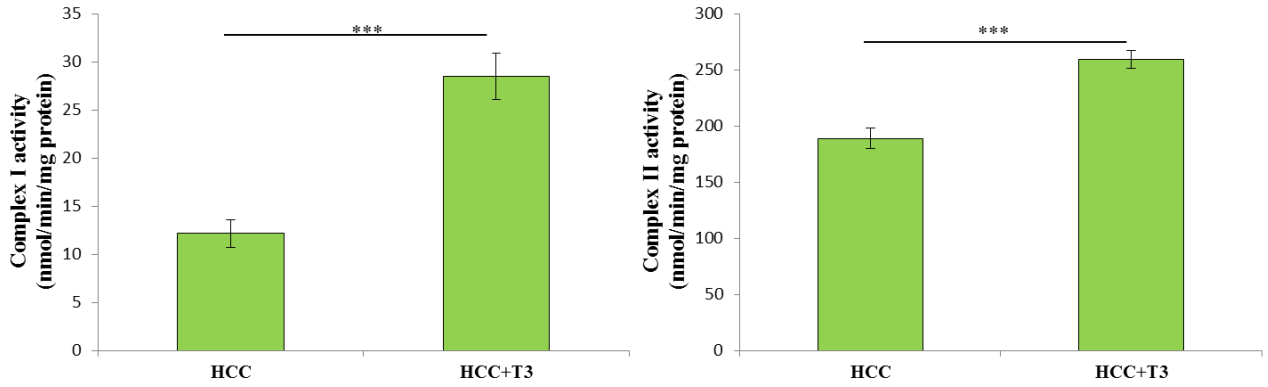

Figure 23 . Enzymatic activity of SDH in HCCs and HCCs+T3. ***P < 0.001.

Repeated cycles of T3 interfere on HCC progression

Having demonstrated that HCCs are able to respond to a short 7-day T3 treatment, we wondered whether repeated cycles of T3 diet could strongly interfere with tumor progression via metabolic switch from Warburg phenotype. To this aim, HCCs-bearing rats from the RH protocol were exposed to 5 cycles of T3 diet (one week every three weeks) and sacrificed 3.5 months thereafter. A group of animals, subjected to the RH protocol but kept in normal diet was included.

At sacrifice, while 100% of the rats exposed to the RH protocol displayed multiple large HCCs, treatment with T3 resulted in an almost complete disappearance of the tumors which were macroscopically evident only in 38% of the animals. Moreover while all untreated animals carried multiple macroscopically evident HCCs, among T3-treated rats, only 15% displayed multiple HCCs (Figure 24). Histological analysis of livers from the untreated group revealed the presence of tumors, ranging from well to poorly differentiated HCCs, in which neoplastic hepatocytes were organized in thick plates or showed a pseudoglandular pattern. On the other hand, the livers of rats exposed to repeated cycles of T3 displayed only smaller and well differentiated HCCs. (Figure 25). These data indicate that thyroid hormone is able to induce a phenotypic regression of advanced neoplastic lesions.

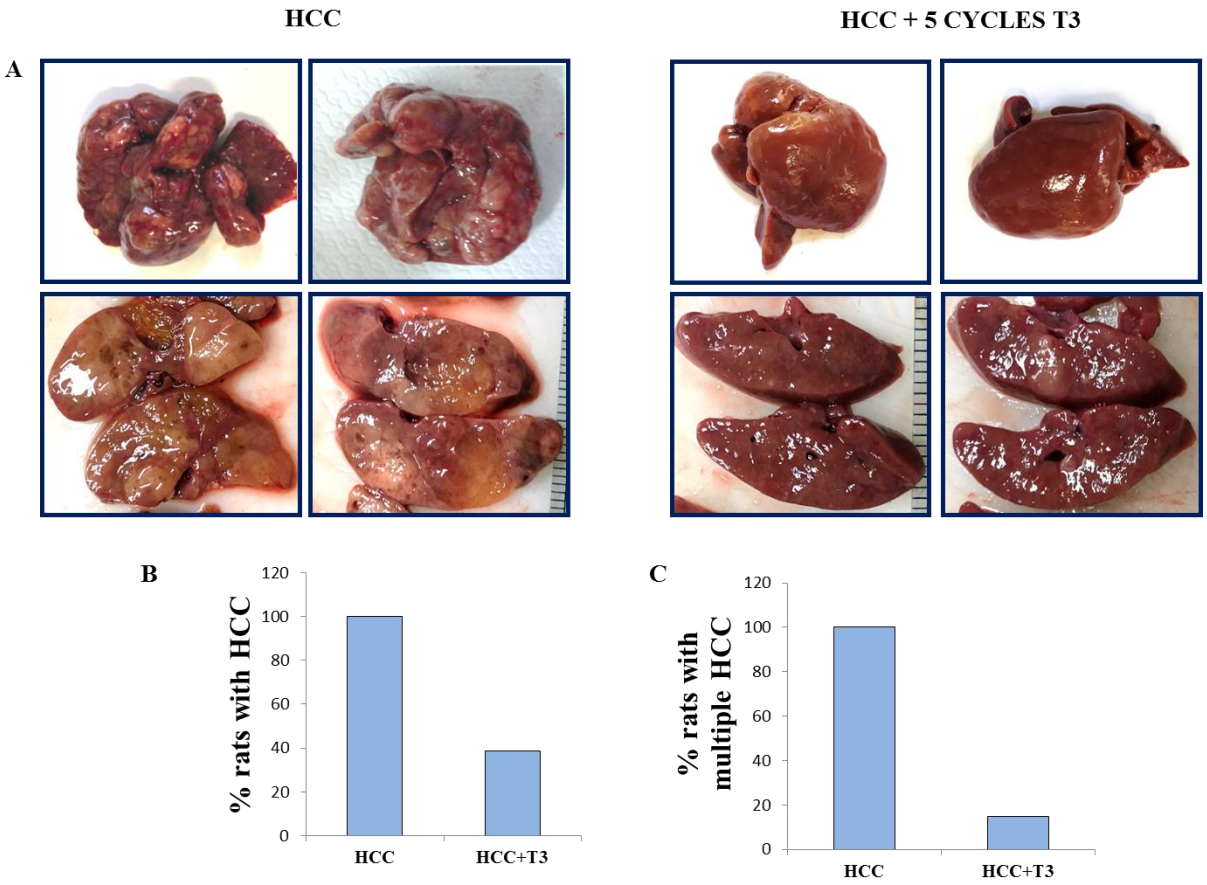

Figure 24 . (A): Representative gross liver images of rats fed basal diet vs. animals fed T3 for 5 repeated cycles. T3 group displays a lower number and burden of tumors. **(B)** and **(C):** percentage of rats showing macroscopically evident and multiple HCCs in T3 and basal diet fed groups.

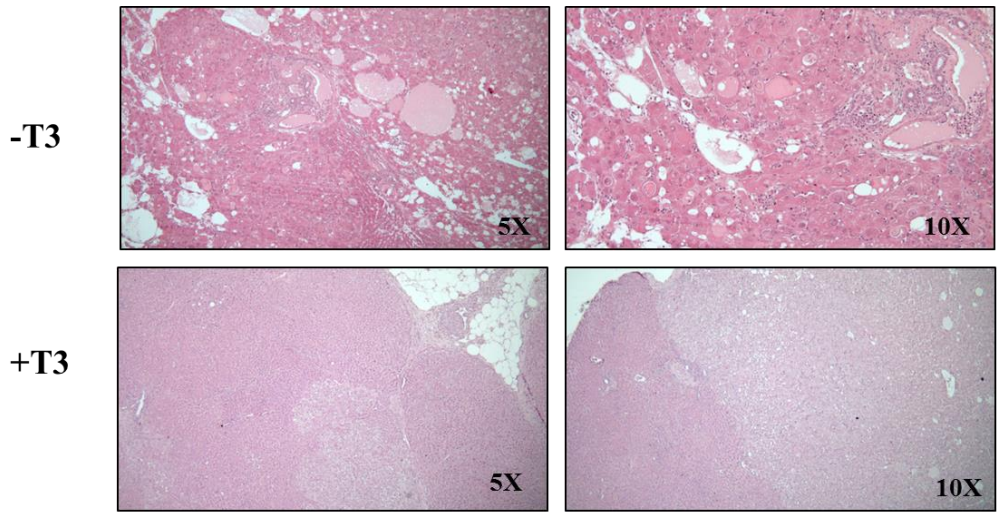

Figure 25 . Histological observation of the tumors by Hematoxylin and Eosin (H&E) staining under light-field microscope with 5x and 10x magnification.

Re-establishment of the T3/TR axis induces regression of HCC and completely reverts the metabolic profile of cancer cells

Five cycles of T3 led to the re-establishment of the T3/TR axis, as shown by a significant increase of *Dio1* and *Spot14* mRNA levels after T3 administration, compared to the very low expression found in HCC of untreated animals (Figure 26 A and B).

Microscopic observations on tumor burden, were confirmed by gene expression analyses. Indeed, a significant down-regulation of neoplastic/stem cell markers, such as *Gst-p* and *Krt-19* mRNA levels were observed in liver sections of T3-treated rats (Figure 26 C and D). Interestingly, IHC on serial sections from livers of T3-treated rats, revealed lesions with different levels of GST-P, but complete disappearance of KRT-19 protein levels (Figure 29). Moreover, even in the livers of T3-treated animals showing macroscopically HCCs, mRNA levels of *Krt-19* were generally very low, suggesting that these tumors underwent a switch towards a more benign phenotype.

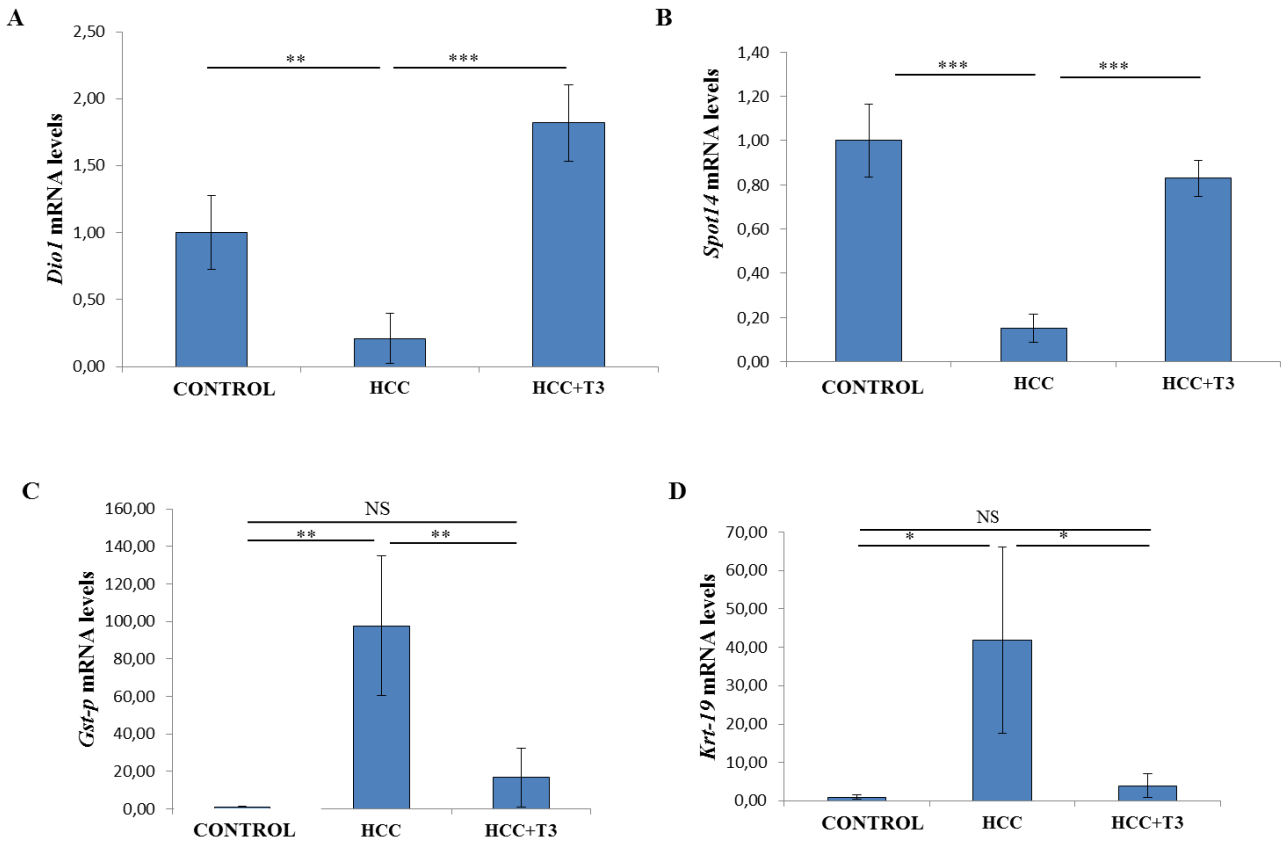

Figure 26 . mRNA expression of *Dio1*, *Spot14*, *Gst-p* and *Krt-19* was assessed by qRT-PCR in controls, HCCs and HCCs+T3. Gene levels were calculated as fold change and normalized using rat *Gapdh* as endogenous control. **P < 0.01; ***P < 0.001; NS: not significant.

These findings prompted us to investigate such T3-dependent anti-tumorigenic effect could be associated to a complete reversion of the metabolic profile of cancer cells. To answer this question, we first analysed proteins involved in glycolysis, PPP and OXPHOS.

Evidence of a return to a normal glycolytic activity in the T3-treated group came from the finding that mRNA and protein levels of *Glut1*, *Hk2* and TIGAR were significantly down-regulated compared to those of HCCs of T3-untreated rats (Figure 27;Figure 28; Figure 29). Five cycles of the hormone induced a significant down-regulation of MCT4 and CS (Figure 28; Figure 29) and reverted the enhanced activation of the PPP found in the tumors, as demonstrated by a return of basal expression levels of *Taldo1*, T*kt* and *G6pd* (Figure 30). Also G6PD activity showed a complete return to normal levels (Figure 30D). In agreement with the notion that *Taldo1*, *Tkt* and *G6pd* are target genes of NRF2, these data were associated to a reduction of the NRF2 pathway activity, as shown by *Nqo1* mRNA and protein levels (Figure 28; Figure 29;Figure 31A).

With regard to mitochondrial respiration, enzymatic activity assays performed on tissues belonging to the T3-treated group also showed an increase of the activity of complex I and II of the respiratory chain. These data were further confirmed by histochemical analysis of serial frozen sections showing a reactivation of SDH activity after T3 treatment (Figure 31B and C). These results indicate that T3 not only reduces glycolysis but also restores OXPHOS.

Taken together, these data provide evidences that T3 is able to revert the metabolic reprogramming observed in both in pre-neoplastic lesions as well as in fully developed HCCs and suggest that reversion of metabolic reprogramming may be responsible for the powerful regression of HCCs.

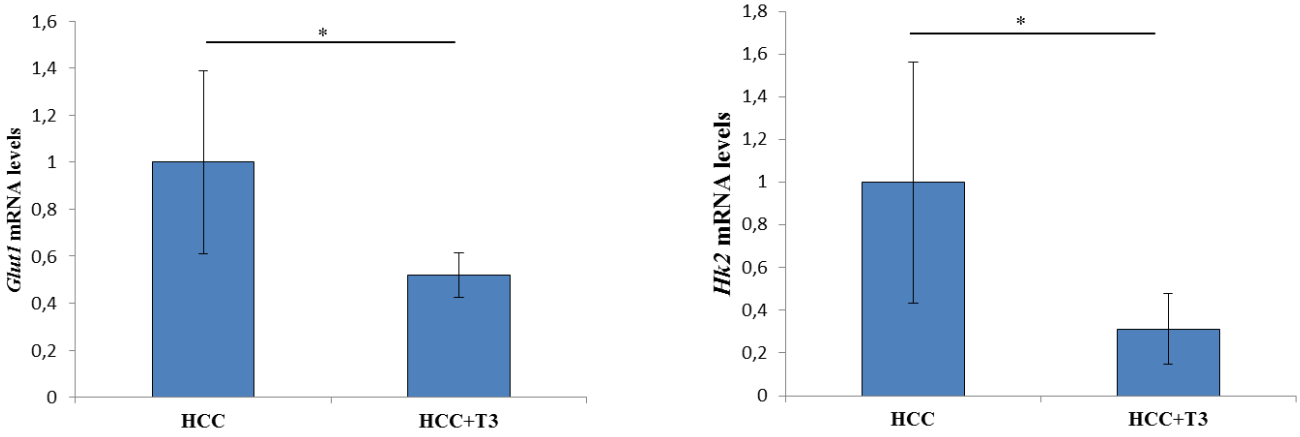

Figure 27 . mRNA expression of *Glut1* and *Hk2* was assessed by qRT-PCR in HCCs and HCCs+T3. Gene levels were calculated as fold change and normalized using rat *Gapdh* as endogenous control. *P < 0.05.

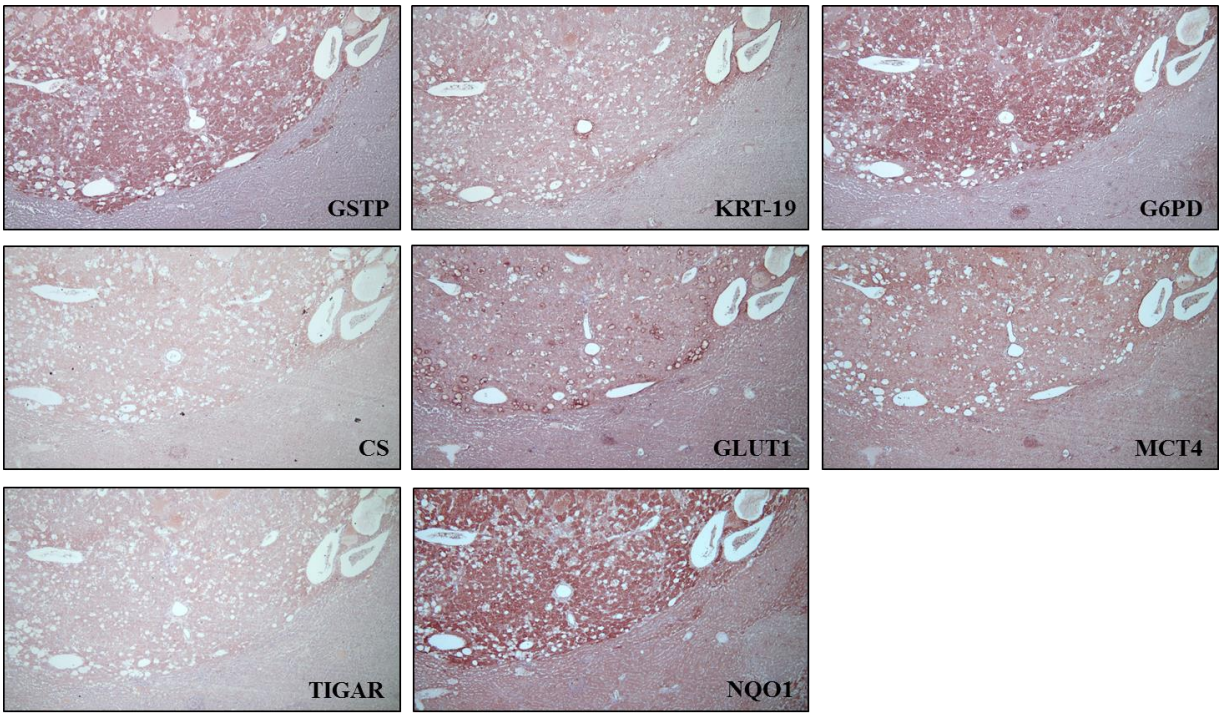

Figure 28 . Immunohistochemical analysis of serial paraffin sections from livers of HCC bearing rats (5x magnification).

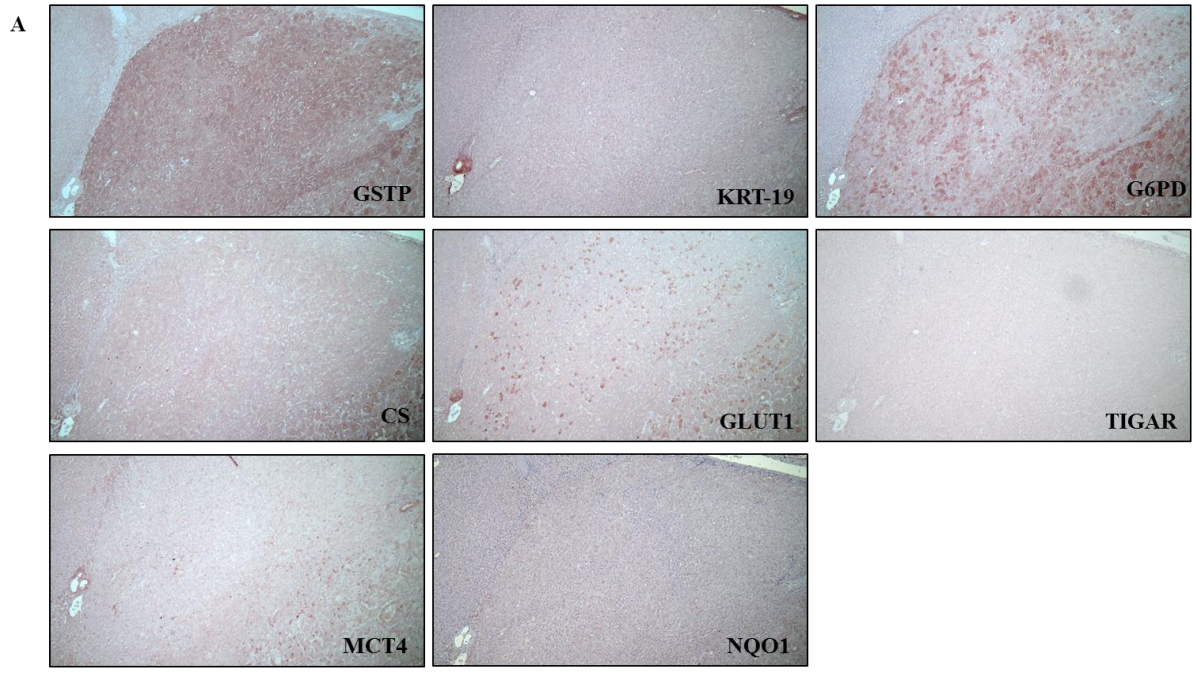

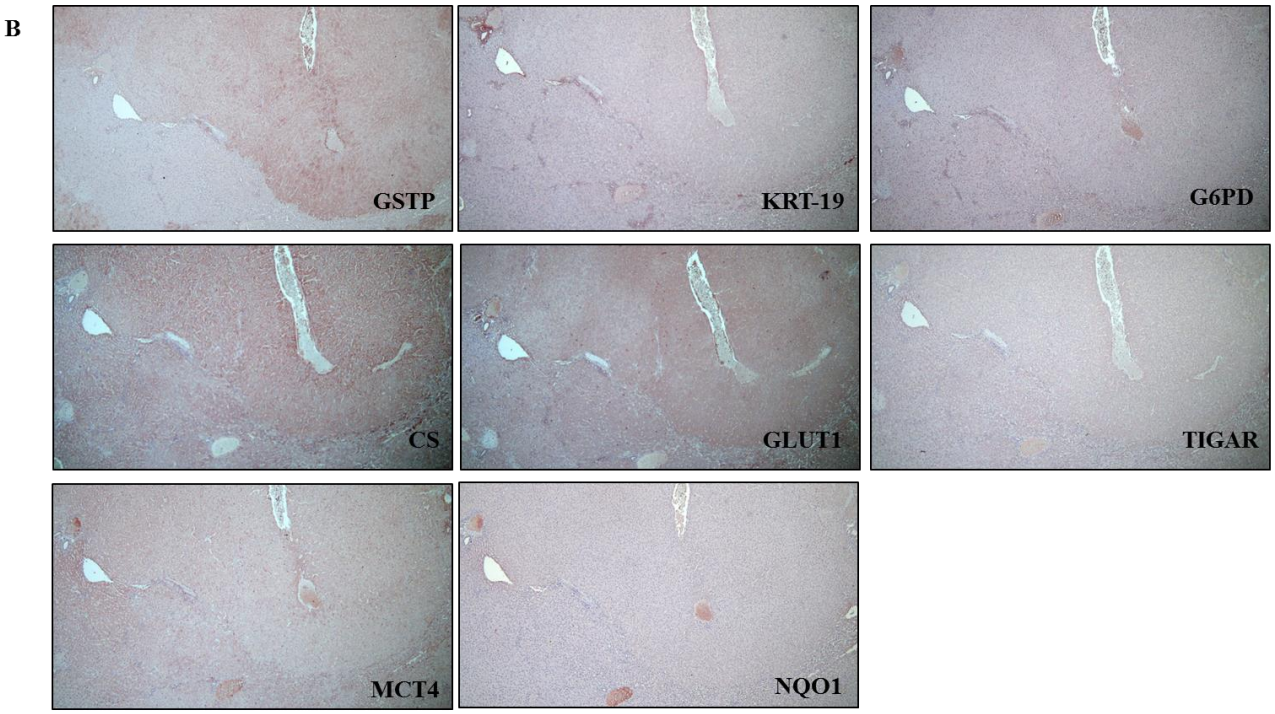

Figure 29 . Immunohistochemical analysis of serial paraffin sections from livers of HCC-bearing rats exposed to 5 repeated cycles of T3 diet showing lesions with different levels of GST-P reduction (A) and (B) (5x magnification).

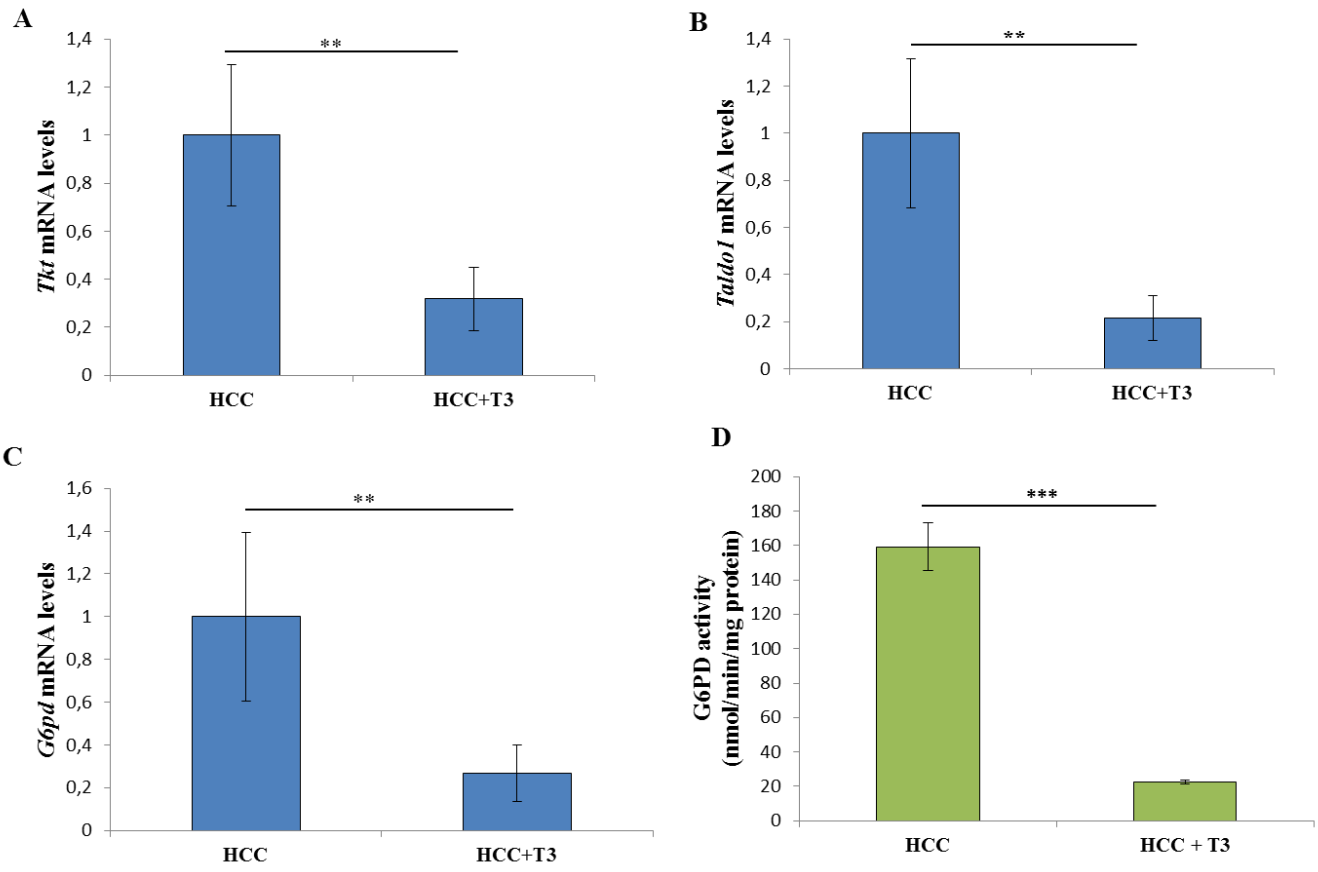

Figure 30 . mRNA expression of *G6pd*, *Taldo1* and *Tkt* was assessed by qRT-PCR in HCCs and HCCs+T3. Gene levels were calculated as fold change and normalized using rat *Gapdh* as endogenous control. **P < 0.01; ***P < 0.001. G6PD activity was measured in HCC and HCC+T3 ***P < 0.001.

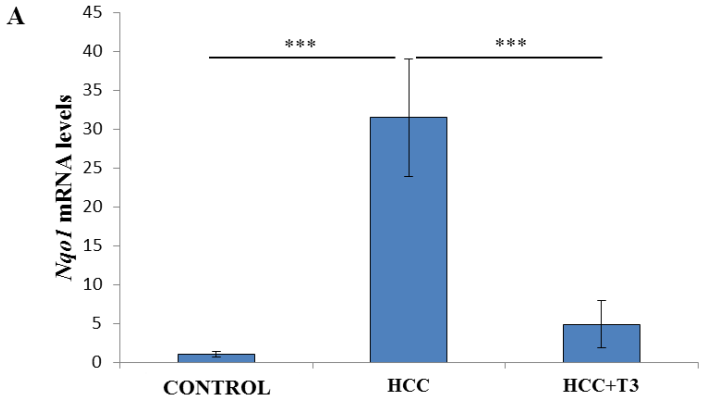

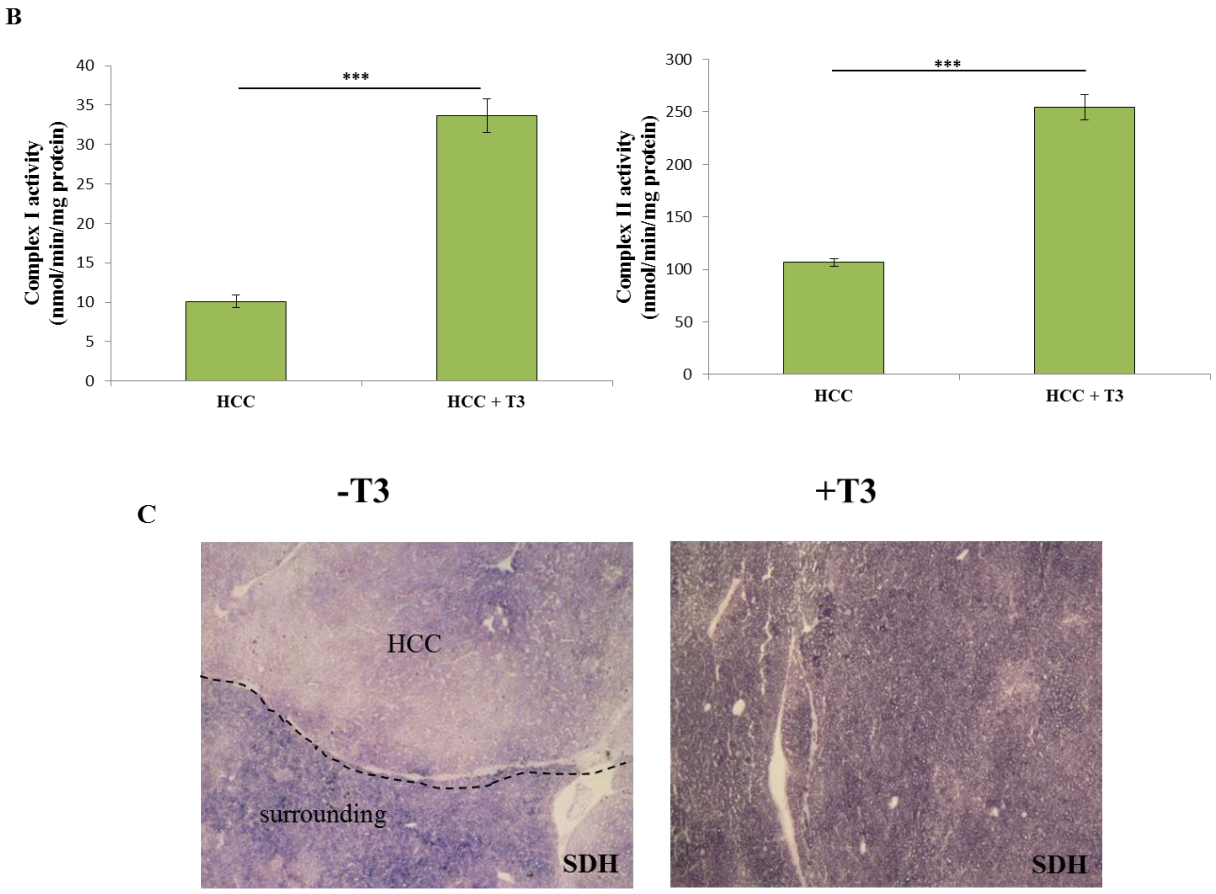

Figure 31 . (A): mRNA expression of *Nqo1* was assessed by qRT-PCR in controls, HCCs and HCCs+T3. Gene levels were calculated as fold change and normalized using rat *Gapdh* as endogenous control. ***P < 0.001. **(B)**: Complex I and Complex II activity were measured in HCC and HCC+T3 ***P < 0.001. **(C)**: Histochemical analysis of SDH activity showing impaired activity in the HCC compared to the surrounding tissue. The activity was restored in the liver from T3-treated rats (magnification 5x).

The metabolic pattern is maintained 4 weeks after T3 withdrawal

Finally, we wondered whether the observed effects of T3 treatment could be maintained even after T3 withdrawal. To this aim, after the fifth cycle of T3 the animals were placed on basal diet and sacrificed 1 month later. One group of rats, exposed to the RH protocol as well, but in the absence of T3 treatment, was included. At sacrifice, all untreated animals carried multiple macroscopically evident HCCs, while the livers of the rats previously treated with T3 showed a significant reduction of tumor burden which was similar to that observed at the end of the 5 cycles treatment (Figure 24; Figure 32).

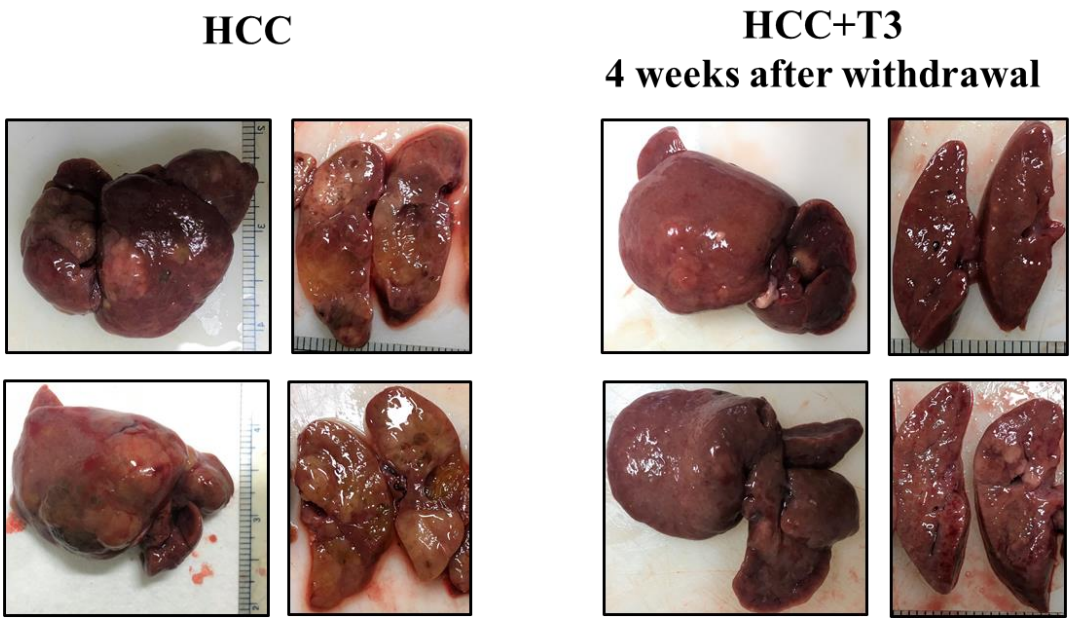

Figure 32 . Representative gross liver images of rats fed basal diet vs. animals fed T3 for 5 repeated cycles and then left in basal diet for 4 weeks.

Accordingly, RT-qPCR analysis of *Krt-19* expression showed a persistent down-regulation in the group previously treated with T3, compared to that of HCCs from rats fed normal diet (Figure 33 A)

As to the T3/TR axis, an increase of *Dio1* and *Spot14* mRNA levels was observed in T3-treated rats. Although the values did not reach statistical significance compared to controls, nevertheless, they were 2-fold higher compared to the untreated HCCs, indicating a low but still detectable and permanent effect on the hormone/receptor axis (Figure 33 B, C, D, E).

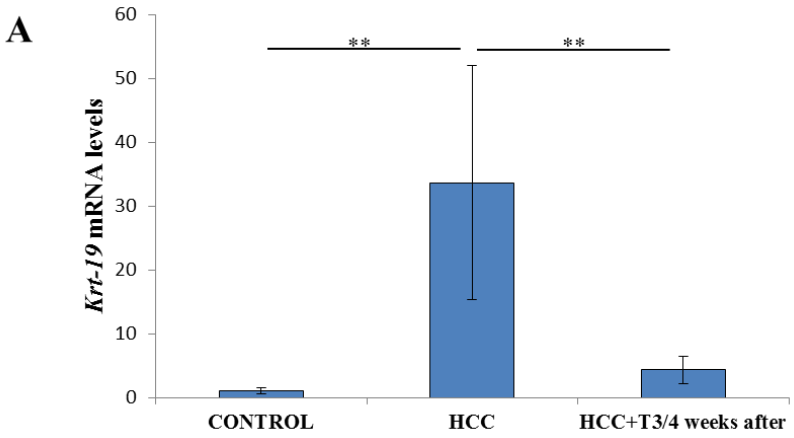

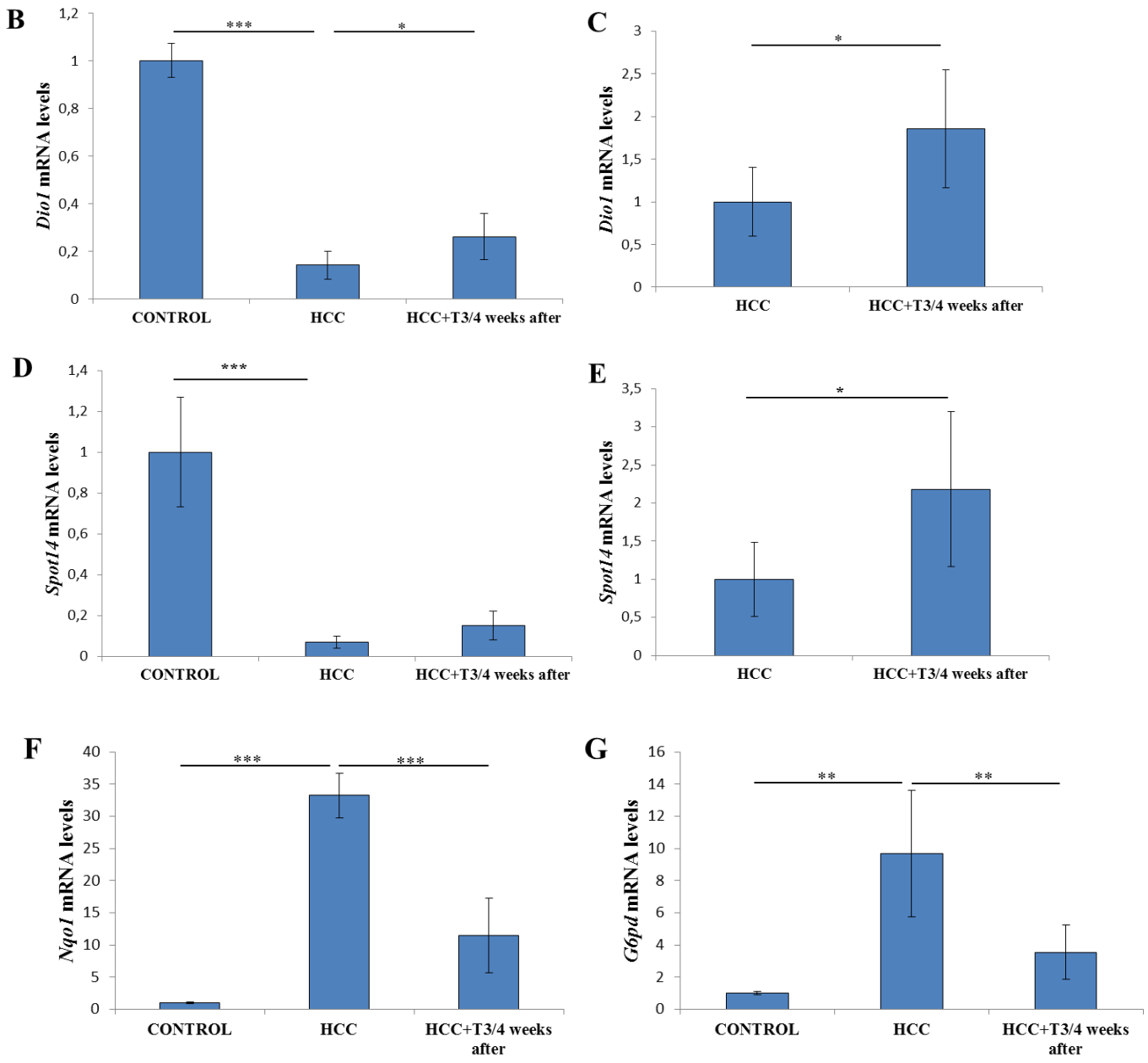

Figure 33 . mRNA expression of *Krt-19, Dio1, Spot14, Nqo1* and *G6pd* were assessed by qRT-PCR in controls, HCCs and HCCs+T3. Gene levels were calculated as fold change and normalized using rat *Gapdh* as endogenous control. ***P < 0.001; **P < 0.01; *P < 0.05.

NRF2 pathway was also found down-regulated compared to HCCs of untreated animals, as shown by gene expression analysis of *Nqo1* and *G6pd* (Figure 33 F, G).

Taken together, these data indicate that the inhibitory effect of T3 treatment on tumor growth was maintained even one month after T3 removal. Further support to this conclusion comes from the finding that the expression of *Krt-19*, a marker of HCC aggressiveness, was strongly down-regulated compared to untreated rats 4 weeks after T3 withdrawal.

CONCLUSIONS

Alterations of different metabolic pathways, such as glycolysis, PPP and mitochondrial respiration have been described in several tumor types [2]. With regard to HCC, Nwosu *et al.*, found more than 600 consistently altered metabolic genes in human HCCs [12]. Moreover, it was shown that in a rat model of hepatocarcinogenesis (R-H model) metabolic reprogramming is a feature observed from very early stages (foci and pre-neoplastic nodules) and persists up to fully developed HCC, suggesting its critical role in HCC onset and progression [62].

Several reports have described the effect of T3 administration on the metabolic behaviour of cancer cells in *in vitro* experiments. In particular, a connection between mitochondrial metabolism and T3 action by modulating Warburg phenomenon has been reported [102]. Indeed, the obtained results suggested that T3 sensitized mitochondrial metabolism in aggressive triple-negative breast cancer cells displaying marked Warburg effect [102]. In addition, using HepG2 cells, Sinha *et al.* showed the ability of T3 to increase mitochondrial function [103], and similar observations showing that T3 treatment leads to an increase in mitochondrial respiration have been recently reported by Chi *et al.*[104].

Since T3 has been shown to exert an inhibitory effect on preneoplastic hepatic cells [90], the present study aimed at investigating whether among the possible mechanisms responsible for the anti-tumorigenic effect of T3 is its capacity of reverting the metabolic profile of cancer cells.

The results of this work showed that a brief T3 (2 to 4 days) treatment of nodules-bearing rats was able to revert the metabolic profile of pre-neoplastic hepatocytes and this effect was observed well before the regression of the nodules (7 days).

Moreover, the results also showed that repeated cycles of T3 to HCCs-bearing rats were able to significantly reduce the tumor burden. Such anti-tumorigenic effect of T3 was also associated to a reversion of the metabolic profile of cancer cells, as demonstrated by the analysis of several genes/enzymes involved in glycolysis, PPP and mitochondrial respiration. Finally, another interesting results was the finding that the effect was maintained at least 1 month after T3 removal, showing a long-lasting effect of T3 and suggesting the irreversibility of the anti-tumoral effect exerted by the hormone.

These data confirmed the anti-neoplastic role of T3 treatment already observed by our laboratory, as well as by other groups [90,105,106].

The novelty of the present study is that T3 is able to induce the regression of HCC even when treatment begins at a time when HCCs are already developed. Considering that HCC in humans is usually diagnosed at late stages and no effective therapeutic strategies are available for such advanced lesions, the ability of T3 to interfere with cancer progression deserves attention in terms of its possible translational use. In this context, it is noteworthy that the anti-tumorigenic and metabolic effect of T3 was maintained for at least 1 month after T3 withdrawal.

In the last decades, the involvement of T3 and TRs in HCC development has been widely described [107]. Indeed, both aberrant expression or mutations of TRs have been frequently observed in HCC [108]. Moreover, a correlation between hypothyroidism and HCC development has been described in human HCC [88,89], suggesting that hypothyroidism may represent a permissive factor for the development of this tumor. Furthermore, recent studies reported a significant down-regulation of TRs, in particular the TRβ1 isoform, in both animal as well as human HCC [76,77]. Conversely, a 7-day treatment with T3 accelerated the regression of chemically-induced rat hepatic pre-neoplastic lesions [90]. In the same line, Chi *et al*. recently demonstrated that T3 exerted a suppressive effect on HCC development in DENA-treated mice via activation of autophagy [105]. The same group further showed the protective effect of T3 on HBV-encoded X protein (HBx)-induced hepatocarcinogenesis [106] . Taken together these reports make possible to postulate that T3/TRs restoration may interfere with HCC progression

In conclusion, the results of the present work showing that T3 is able to induce the regression of HCC even when treatment begins at a time when HCCs are already developed may provide a scientific basis for future clinical applications aimed at counteracting the progression of neoplastic hepatocytes by rescuing the T3/TR axis and modifying their metabolic profile.

T3-associated undesired side effects such as tachycardia, heart failure and other symptoms may preclude clinical use of the thyroid hormone. Therefore, our future studies will investigate if the same anti-tumorigenic and metabolic effect could be exerted also by T3 analogs, devoid of T3 side effects. To this aim, we will perform experiments using recently developed thyroid hormone derivatives that display receptor subtype-selective activities [109].

As to the possible translational value of our present findings, in order to directly establish the possible use of T3/analogs in human HCC therapy, we will perform experiments on HCC patient-derived xenograft (PDX), at present one of the most powerful models for investigating the effect of therapeutic drugs on human tumors.

REFERENCES

1. Hanahan D, Weinberg RA. Hallmarks of cancer: the next generation. Cell. 2011 Mar 4;144(5):646–74.

2. Pavlova NN, Thompson CB. The Emerging Hallmarks of Cancer Metabolism. Cell Metab. 2016 Jan 12;23(1):27–47.

3. Warburg O, Wind F, Negelein E. The metabolism of tumor in the body. J Gen Physiol. 1927 Mar 7;8(6):519–30.

4. Warburg O. On the Origin of Cancer Cells. Science. 1956;123(3191):309–14.

5. Weinhouse S, Warburg O, Burk D, Schade AL. On Respiratory Impairment in Cancer Cells. Science. 1956 Aug 10;124(3215):267–72.

6. Weinhouse S. The Warburg hypothesis fifty years later. Z Für Krebsforsch Klin Onkol. 1976 Jan 1;87(2):115–26.

7. Moreno-Sánchez R, Rodríguez-Enríquez S, Marín-Hernández A, Saavedra E. Energy metabolism in tumor cells. FEBS J. 2007 Mar 1;274(6):1393–418.

8. DeBerardinis RJ, Lum JJ, Hatzivassiliou G, Thompson CB. The Biology of Cancer: Metabolic Reprogramming Fuels Cell Growth and Proliferation. Cell Metab. 2008 Jan 1;7(1):11–20.

9. Gatenby RA, Gillies RJ. Why do cancers have high aerobic glycolysis? Nat Rev Cancer. 2004 Nov;4(11):891–9.

10. Heiden MGV, Cantley LC, Thompson CB. Understanding the Warburg Effect: The Metabolic Requirements of Cell Proliferation. Science. 2009 May 22;324(5930):1029–33.

11. Son J, Lyssiotis CA, Ying H, Wang X, Hua S, Ligorio M, et al. Glutamine supports pancreatic cancer growth through a KRAS-regulated metabolic pathway. Nature. 2013 Apr;496(7443):101–5.

12. Nwosu ZC, Megger DA, Hammad S, Sitek B, Roessler S, Ebert MP, et al. Identification of the Consistently Altered Metabolic Targets in Human Hepatocellular Carcinoma. Cell Mol Gastroenterol Hepatol. 2017 Sep 1;4(2):303-323.e1.

13. Liu T, Yin H. PDK1 promotes tumor cell proliferation and migration by enhancing the Warburg effect in non-small cell lung cancer. Oncol Rep. 2017 Jan 1;37(1):193–200.

14. Nicklin P, Bergman P, Zhang B, Triantafellow E, Wang H, Nyfeler B, et al. Bidirectional Transport of Amino Acids Regulates mTOR and Autophagy. Cell. 2009 Feb 6;136(3):521–34.

15. Hanahan D, Weinberg RA. The Hallmarks of Cancer. Cell. 2000 Jan 7;100(1):57–70.

16. Wieman HL, Wofford JA, Rathmell JC, Margolis B. Cytokine Stimulation Promotes Glucose Uptake via Phosphatidylinositol-3 Kinase/Akt Regulation of Glut1 Activity and Trafficking. Mol Biol Cell. 2007 Feb 14;18(4):1437–46.

17. Barthel A, Okino ST, Liao J, Nakatani K, Li J, Whitlock JP, et al. Regulation of GLUT1 Gene Transcription by the Serine/Threonine Kinase Akt1. J Biol Chem. 1999 Jul 16;274(29):20281–6.

18. Murakami T, Nishiyama T, Shirotani T, Shinohara Y, Kan M, Ishii K, et al. Identification of two enhancer elements in the gene encoding the type 1 glucose transporter from the mouse which are responsive to serum, growth factor, and oncogenes. J Biol Chem. 1992 May 5;267(13):9300–6.

19. Gottlob K, Majewski N, Kennedy S, Kandel E, Robey RB, Hay N. Inhibition of early apoptotic events by Akt/PKB is dependent on the first committed step of glycolysis and mitochondrial hexokinase. Genes Dev. 2001 Jan 6;15(11):1406–18.

20. Deprez J, Vertommen D, Alessi DR, Hue L, Rider MH. Phosphorylation and Activation of Heart 6-Phosphofructo-2-kinase by Protein Kinase B and Other Protein Kinases of the Insulin Signaling Cascades. J Biol Chem. 1997 Nov 7;272(28):17269–75.

21. Wang R, Dillon CP, Shi LZ, Milasta S, Carter R, Finkelstein D, et al. The Transcription Factor Myc Controls Metabolic Reprogramming upon T Lymphocyte Activation. Immunity. 2011 Dec 23;35(6):871–82.

22. Eberhardy SR, Farnham PJ. c-Myc Mediates Activation of the cad Promoter via a Post-RNA Polymerase II Recruitment Mechanism. J Biol Chem. 2001 Dec 21;276(51):48562–71.

23. Gao P, Tchernyshyov I, Chang T-C, Lee Y-S, Kita K, Ochi T, et al. c-Myc suppression of miR-23a/b enhances mitochondrial glutaminase expression and glutamine metabolism. Nature. 2009 Apr;458(7239):762–5.

24. Frezza C. The role of mitochondria in the oncogenic signal transduction. Int J Biochem Cell Biol. 2014 Mar 1;48:11–7.

25. Yang M, Soga T, Pollard PJ. Oncometabolites: linking altered metabolism with cancer. J Clin Invest. 2013 Sep;123(9):3652–8.

26. Cairns RA, Mak TW. Oncogenic Isocitrate Dehydrogenase Mutations: Mechanisms, Models, and Clinical Opportunities. Cancer Discov. 2013 Jul 1;3(7):730–41.

27. Gasparre G, Hervouet E, de Laplanche E, Demont J, Pennisi LF, Colombel M, et al. Clonal expansion of mutated mitochondrial DNA is associated with tumor formation and complex I deficiency in the benign renal oncocytoma. Hum Mol Genet. 2008 Apr 1;17(7):986–95.

28. Abu-Amero KK, Alzahrani AS, Zou M, Shi Y. High frequency of somatic mitochondrial DNA mutations in human thyroid carcinomas and complex I respiratory defect in thyroid cancer cell lines. Oncogene. 2005 Feb;24(8):1455–60.

29. Petros JA, Baumann AK, Ruiz-Pesini E, Amin MB, Sun CQ, Hall J, et al. mtDNA mutations increase tumorigenicity in prostate cancer. Proc Natl Acad Sci. 2005 Jan 18;102(3):719–24.

30. Kowalik MA, Columbano A, Perra A. Emerging Role of the Pentose Phosphate Pathway in Hepatocellular Carcinoma. Front Oncol [Internet]. 2017 [cited 2018 Nov 17];7. Available from: https://www.frontiersin.org/articles/10.3389/fonc.2017.00087/full

31. Wang C, Guo K, Gao D, Kang X, Jiang K, Li Y, et al. Identification of transaldolase as a novel serum biomarker for hepatocellular carcinoma metastasis using xenografted mouse model and clinic samples. Cancer Lett. 2011 Dec 27;313(2):154–66.

32. Xu X, Hausen A zur, Coy JF, Löchelt M. Transketolase-like protein 1 (TKTL1) is required for rapid cell growth and full viability of human tumor cells. Int J Cancer. 2009 Mar 15;124(6):1330–7.

33. Fan J, Ye J, Kamphorst JJ, Shlomi T, Thompson CB, Rabinowitz JD. Quantitative flux analysis reveals folate-dependent NADPH production. Nature. 2014 Jun;510(7504):298–302.

34. Bensaad K, Tsuruta A, Selak MA, Vidal MNC, Nakano K, Bartrons R, et al. TIGAR, a p53-Inducible Regulator of Glycolysis and Apoptosis. Cell. 2006 Jul 14;126(1):107–20.

35. Lee P, Vousden KH, Cheung EC. TIGAR, TIGAR, burning bright. Cancer Metab. 2014 Jan 3;2(1):1.

36. Wong CC-L, Au SL-K, Tse AP-W, Xu IM-J, Lai RK-H, Chiu DK-C, et al. Switching of Pyruvate Kinase Isoform L to M2 Promotes Metabolic Reprogramming in Hepatocarcinogenesis. PLOS ONE. 2014 Dec 26;9(12):e115036.

37. Dong G, Mao Q, Xia W, Xu Y, Wang J, Xu L, et al. PKM2 and cancer: The function of PKM2 beyond glycolysis. Oncol Lett. 2016 Mar;11(3):1980–6.

38. Christofk HR, Vander Heiden MG, Wu N, Asara JM, Cantley LC. Pyruvate kinase M2 is a phosphotyrosine-binding protein. Nature. 2008 Mar;452(7184):181–6.

39. DeBerardinis RJ, Mancuso A, Daikhin E, Nissim I, Yudkoff M, Wehrli S, et al. Beyond aerobic glycolysis: Transformed cells can engage in glutamine metabolism that exceeds the requirement for protein and nucleotide synthesis. Proc Natl Acad Sci. 2007 Dec 4;104(49):19345–50.

40. Hay N. Reprogramming glucose metabolism in cancer: can it be exploited for cancer therapy? Nat Rev Cancer. 2016 Oct;16(10):635–49.

41. Bray F, Ferlay J, Laversanne M, Brewster DH, Mbalawa CG, Kohler B, et al. Cancer Incidence in Five Continents: Inclusion criteria, highlights from Volume X and the global status of cancer registration. Int J Cancer. 2015 Nov 1;137(9):2060–71.

42. Llovet JM, Zucman-Rossi J, Pikarsky E, Sangro B, Schwartz M, Sherman M, et al. Hepatocellular carcinoma. Nat Rev Dis Primer. 2016 Apr 14;2:16018.

43. New Global Cancer Data: GLOBOCAN 2018 | UICC [Internet]. [cited 2018 Nov 20]. Available from: https://www.uicc.org/new-global-cancer-data-globocan-2018

44. El–Serag HB, Rudolph KL. Hepatocellular Carcinoma: Epidemiology and Molecular Carcinogenesis. Gastroenterology. 2007 Jun 1;132(7):2557–76.

45. McGlynn KA, Petrick JL, London WT. Global Epidemiology of Hepatocellular Carcinoma: An Emphasis on Demographic and Regional Variability. Clin Liver Dis. 2015 May 1;19(2):223–38.

46. Kiyosawa K, Sodeyama T, Tanaka E, Gibo Y, Yoshizawa K, Nakano Y, et al. Interrelationship of blood transfusion, non-A, non-B hepatitis and hepatocellular carcinoma: Analysis by detection of antibody to hepatitis C virus. Hepatology. 1990 Oct 1;12(4):671–5.

47. McMahon BJ. Epidemiology and Natural History of Hepatitis B. Semin Liver Dis. 2005 Feb;25(S 1):3–8.

48. Trevisani F, Cantarini MC, Wands JR, Bernardi M. Recent advances in the natural history of hepatocellular carcinoma. Carcinogenesis. 2008 Jul 1;29(7):1299–305.

49. Thorgeirsson SS, Grisham JW. Molecular pathogenesis of human hepatocellular carcinoma. Nat Genet. 2002 Aug;31(4):339–46.

50. Yuen M-F, Cheng C-C, Lauder IJ, Lam S-K, Ooi CG, Lai C-L. Early detection of hepatocellular carcinoma increases the chance of treatment: Hong Kong experience. Hepatology. 2000 Feb 1;31(2):330–5.

51. Trevisani F, D'Intino PE, Caraceni P, Pizzo M, Stefanini GF, Mazziotti A, et al. Etiologic factors and clinical presentation of hepatocellular carcinoma. Differences between cirrhotic and noncirrhotic Italian patient. Cancer. 1995 May 1;75(9):2220–32.

52. Pons-Renedo F, Llovet JM. Hepatocellular Carcinoma: A Clinical Update. Medscape [Internet]. 2003 Jul 22 [cited 2018 Nov 17];5(3). Available from: http://www.medscape.com/viewarticle/457796

53. Bruix J, Sherman M. Management of hepatocellular carcinoma. Hepatology. 2005 Nov 1;42(5):1208–36.

54. Llovet JM, Ricci S, Mazzaferro V, Hilgard P, Gane E, Blanc J-F, et al. Sorafenib in Advanced Hepatocellular Carcinoma. N Engl J Med [Internet]. 2009 Jul 17 [cited 2018 Nov 17]; Available from: https://www.nejm.org/doi/10.1056/NEJMoa0708857?url_ver=Z39.88-2003&rfr_id=ori%3Arid%3Acrossref.org&rfr_dat=cr_pub%3Dwww.ncbi.nlm.nih.gov

55. Bruix J, Qin S, Merle P, Granito A, Huang Y-H, Bodoky G, et al. Regorafenib for patients with hepatocellular carcinoma who progressed on sorafenib treatment (RESORCE): a randomised, double-blind, placebo-controlled, phase 3 trial. The Lancet. 2017 Jan 7;389(10064):56–66.

56. Finn RS, Merle P, Granito A, Huang Y-H, Bodoky G, Pracht M, et al. Outcomes of sequential treatment with sorafenib followed by regorafenib for HCC: Additional analyses from the phase III RESORCE trial. J Hepatol. 2018 Aug 1;69(2):353–8.

57. Hu J, Locasale JW, Bielas JH, O'Sullivan J, Sheahan K, Cantley LC, et al. Heterogeneity of tumor-induced gene expression changes in the human metabolic network. Nat Biotechnol. 2013 Jun;31(6):522–9.

58. Baba M, Yamamoto R, Iishi H, Tatsuta M, Wada A. Role of glucose-6-phosphate dehydrogenase on enhanced proliferation of pre-neoplastic and neoplastic cells in rat liver induced by n-nitrosomorpholine. Int J Cancer. 1989 May 15;43(5):892–5.

59. Stumpf H, Bannasch P. Overexpression of glucose-6-phosphate-dehydrogenase in rat hepatic preneoplasia and neoplasia. Int J Oncol. 1994 Dec 1;5(6):1255–60.

60. Yuneva MO, Fan TWM, Allen TD, Higashi RM, Ferraris DV, Tsukamoto T, et al. The Metabolic Profile of Tumors Depends on Both the Responsible Genetic Lesion and Tissue Type. Cell Metab. 2012 Feb 8;15(2):157–70.

61. von Morze C, Larson PEZ, Hu S, Yoshihara HAI, Bok RA, Goga A, et al. Investigating tumor perfusion and metabolism using multiple hyperpolarized (13)C compounds: HP001, pyruvate and urea. Magn Reson Imaging. 2012 Apr;30(3):305–11.

62. Kowalik MA, Guzzo G, Morandi A, Perra A, Menegon S, Masgras I, et al. Metabolic reprogramming identifies the most aggressive lesions at early phases of hepatic carcinogenesis. Oncotarget. 2016 Apr 7;7(22):32375–93.

63. Solt DB, Medline A, Farber E. Rapid Emergence of Carcinogen-Induced Hyperplastic Lesions in a New Model for the Sequential Analysis of Liver Carcinogenesis. Am J Pathol. 1977 Sep;88(3):595–618.

64. Sato K, Satoh K, Tsuchida S, Hatayama I, Shen H, Yokoyama Y, et al. Specific Expression of Glutathione S-transferase Pi Forms in (Pre)neoplastic Tissues: Their Properties and Functions. Tohoku J Exp Med. 1992;168(2):97–103.

65. Lee J-S, Heo J, Libbrecht L, Chu I-S, Kaposi-Novak P, Calvisi DF, et al. A novel prognostic subtype of human hepatocellular carcinoma derived from hepatic progenitor cells. Nat Med. 2006 Apr;12(4):410–6.

66. Yang X-R, Xu Y, Yu B, Zhou J, Qiu S-J, Shi G-M, et al. High expression levels of putative hepatic stem/progenitor cell biomarkers related to tumour angiogenesis and poor prognosis of hepatocellular carcinoma. Gut. 2010 Jul 1;59(7):953–62.

67. Kowalik MA, Sulas P, Ledda-Columbano GM, Giordano S, Columbano A, Perra A. Cytokeratin-19 positivity is acquired along cancer progression and does not predict cell origin in rat hepatocarcinogenesis. Oncotarget. 2015 Oct 6;6(36):38749–63.

68. Andersen JB, Loi R, Perra A, Factor VM, Ledda-Columbano GM, Columbano A, et al. Progenitor-derived hepatocellular carcinoma model in the rat. Hepatology. 2010 Apr 1;51(4):1401–9.

69. Dietrich JW, Landgrafe G, Fotiadou EH. TSH and Thyrotropic Agonists: Key Actors in Thyroid Homeostasis. J Thyroid Res [Internet]. 2012 [cited 2018 Nov 17]; Available from: https://www.hindawi.com/journals/jtr/2012/351864/abs/

70. Bianco AC, Salvatore D, Gereben B, Berry MJ, Larsen PR. Biochemistry, Cellular and Molecular Biology, and Physiological Roles of the Iodothyronine Selenodeiodinases. Endocr Rev. 2002 Feb 1;23(1):38–89.

71. Davis PJ, Goglia F, Leonard JL. Nongenomic actions of thyroid hormone. Nat Rev Endocrinol. 2016 Feb;12(2):111–21.

72. Bradley DJ, Towle HC, Young WS. Spatial and temporal expression of alpha- and beta-thyroid hormone receptor mRNAs, including the beta 2-subtype, in the developing mammalian nervous system. J Neurosci. 1992 Jun 1;12(6):2288–302.

73. Cheng S-Y, Leonard JL, Davis PJ. Molecular Aspects of Thyroid Hormone Actions. Endocr Rev. 2010 Apr 1;31(2):139–70.

74. Li Z, Meng ZH, Chandrasekaran R, Kuo W-L, Collins CC, Gray JW, et al. Biallelic Inactivation of the Thyroid Hormone Receptor β1 Gene in Early Stage Breast Cancer. Cancer Res. 2002 Apr 1;62(7):1939–43.

75. Hörkkö TT, Tuppurainen K, George SM, Jernvall P, Karttunen TJ, Mäkinen MJ. Thyroid hormone receptor β1 in normal colon and colorectal cancer–association with differentiation, polypoid growth type and K-ras mutations. Int J Cancer. 2006 Apr 1;118(7):1653–9.

76. Liao C-H, Yeh C-T, Huang Y-H, Wu S-M, Chi H-C, Tsai M-M, et al. Dickkopf 4 positively regulated by the thyroid hormone receptor suppresses cell invasion in human hepatoma cells. Hepatology. 2012 Mar 1;55(3):910–20.

77. Kamiya Y, Puzianowska-Kuznicka M, McPhie P, Nauman J, Cheng S, Nauman A. Expression of mutant thyroid hormone nuclear receptors is associated with human renal clear cell carcinoma. Carcinogenesis. 2002 Jan 1;23(1):25–33.

78. Puzianowska-Kuznicka M, Krystyniak A, Madej A, Cheng S-Y, Nauman J. Functionally Impaired TR Mutants Are Present in Thyroid Papillary Cancer. J Clin Endocrinol Metab. 2002 Mar 1;87(3):1120–8.

79. Martínez-Iglesias O, Garcia-Silva S, Tenbaum SP, Regadera J, Larcher F, Paramio JM, et al. Thyroid Hormone Receptor β1 Acts as a Potent Suppressor of Tumor Invasiveness and Metastasis. Cancer Res. 2009 Jan 15;69(2):501–9.

80. Frau C, Loi R, Petrelli A, Perra A, Menegon S, Kowalik MA, et al. Local hypothyroidism favors the progression of preneoplastic lesions to hepatocellular carcinoma in rats. Hepatology. 2015 Jan 1;61(1):249–59.

81. Martínez-Iglesias OA, Alonso-Merino E, Gómez-Rey S, Velasco-Martín JP, Orozco RM, Luengo E, et al. Autoregulatory loop of nuclear corepressor 1 expression controls invasion, tumor growth, and metastasis. Proc Natl Acad Sci. 2016 Jan 19;113(3):E328–37.

82. Lin K-H, Shieh H-Y, Chen S-L, Hsu H-C. Expression of mutant thyroid hormone nuclear receptors in human hepatocellular carcinoma cells. Mol Carcinog. 1999 Sep 1;26(1):53–61.

83. Lin KH, Zhu XG, Shieh HY, Hsu HC, Chen ST, McPhie P, et al. Identification of naturally occurring dominant negative mutants of thyroid hormone alpha 1 and beta 1 receptors in a human hepatocellular carcinoma cell line. Endocrinology. 1996 Oct 1;137(10):4073–81.

84. cBioPortal for Cancer Genomics [Internet]. [cited 2018 Nov 20]. Available from: http://www.cbioportal.org/

85. Villanueva A, Portela A, Sayols S, Battiston C, Hoshida Y, Méndez-González J, et al. DNA methylation-based prognosis and epidrivers in hepatocellular carcinoma. Hepatology. 2015 Jun 1;61(6):1945–56.

86. Boguslawska J, Wojcicka A, Piekielko-Witkowska A, Master A, Nauman A. MiR-224 Targets the 3′UTR of Type 1 5′-Iodothyronine Deiodinase Possibly Contributing to Tissue Hypothyroidism in Renal Cancer. PLOS ONE. 2011 Sep 2;6(9):e24541.

87. Giordano S, Columbano A. MicroRNAs: New tools for diagnosis, prognosis, and therapy in hepatocellular carcinoma? Hepatology. 2013 Feb 1;57(2):840–7.

88. Hassan MM, Kaseb A, Li D, Patt YZ, Vauthey J-N, Thomas MB, et al. Association between hypothyroidism and hepatocellular carcinoma: A case-control study in the United States. Hepatology. 2009 May 1;49(5):1563–70.

89. Reddy A, Dash C, Leerapun A, Mettler TA, Stadheim LM, Lazaridis KN, et al. Hypothyroidism: A Possible Risk Factor for Liver Cancer in Patients With No Known Underlying Cause of Liver Disease. Clin Gastroenterol Hepatol. 2007 Jan 1;5(1):118–23.

90. Ledda-Columbano GM, Perra A, Loi R, Shinozuka H, Columbano A. Cell Proliferation Induced by Triiodothyronine in Rat Liver Is Associated with Nodule Regression and Reduction of Hepatocellular Carcinomas. Cancer Res. 2000 Feb 1;60(3):603–9.

91. Rutenburg AM, Kim H, Fischbein JW, Hanker JS, Wasserkrug HL, Seligman AM. Histochemical and ultrastructural demonstration of gamma-glutamyl transpeptidase activity. J Histochem Cytochem. 1969 Aug;17(8):517–26.

92. Wohlrab F. Specificity of the histochemical demonstration of nucleoside phosphatases by the Wachstein-Meisel technic. Z Mikrosk Anat Forsch. 1971;83(1):90–108.

93. Friedrich-Freksa H, Gössner W, Börner P. Histochemical investigations of carcinogenesis in rat liver after continuous application of diethylnitrosamine. Z Krebsforsch. 1969;72(3):226–39.

94. Cho J-H, Kim G-Y, Mansfield BC, Chou JY. Hepatic glucose-6-phosphatase-α deficiency leads to metabolic reprogramming in glycogen storage disease type Ia. Biochem Biophys Res Commun. 2018 Apr 15;498(4):925–31.

95. Feng X, Jiang Y, Meltzer P, Yen PM. Thyroid Hormone Regulation of Hepatic Genes in Vivo Detected by Complementary DNA Microarray. Mol Endocrinol. 2000 Jul 1;14(7):947–55.

96. Chen J-Q, Russo J. Dysregulation of glucose transport, glycolysis, TCA cycle and glutaminolysis by oncogenes and tumor suppressors in cancer cells. Biochim Biophys Acta BBA - Rev Cancer. 2012 Dec 1;1826(2):370–84.

97. Kwee SA, Hernandez B, Chan O, Wong L. Choline Kinase Alpha and Hexokinase-2 Protein Expression in Hepatocellular Carcinoma: Association with Survival. PLOS ONE. 2012 Oct 5;7(10):e46591.

98. Mitsuishi Y, Taguchi K, Kawatani Y, Shibata T, Nukiwa T, Aburatani H, et al. Nrf2 Redirects Glucose and Glutamine into Anabolic Pathways in Metabolic Reprogramming. Cancer Cell. 2012 Jul 10;22(1):66–79.

99. Petrelli A, Perra A, Cora D, Sulas P, Menegon S, Manca C, et al. MicroRNA/gene profiling unveils early molecular changes and nuclear factor erythroid related factor 2 (NRF2) activation in a rat model recapitulating human hepatocellular carcinoma (HCC). Hepatology. 2014 Jan 1;59(1):228–41.

100. Parks SK, Chiche J, Pouysségur J. Disrupting proton dynamics and energy metabolism for cancer therapy. Nat Rev Cancer. 2013 Sep;13(9):611–23.

101. Gao H-J, Zhao M-C, Zhang Y-J, Zhou D-S, Xu L, Li G-B, et al. Monocarboxylate transporter 4 predicts poor prognosis in hepatocellular carcinoma and is associated with cell proliferation and migration. J Cancer Res Clin Oncol. 2015 Jul 1;141(7):1151–62.

102. Suhane S, Ramanujan VK. Thyroid hormone differentially modulates Warburg phenotype in breast cancer cells. Biochem Biophys Res Commun. 2011 Oct 14;414(1):73–8.

103. Sinha RA, Singh BK, Zhou J, Wu Y, Farah BL, Ohba K, et al. Thyroid hormone induction of mitochondrial activity is coupled to mitophagy via ROS-AMPK-ULK1 signaling. Autophagy. 2015 Aug 3;11(8):1341–57.

104. Chi H-C, Chen S-L, Lin S-L, Tsai C-Y, Chuang W-Y, Lin Y-H, et al. Thyroid hormone protects hepatocytes from HBx-induced carcinogenesis by enhancing mitochondrial turnover. Oncogene. 2017 Sep;36(37):5274–84.

105. Chi H-C, Chen S-L, Tsai C-Y, Chuang W-Y, Huang Y-H, Tsai M-M, et al. Thyroid hormone suppresses hepatocarcinogenesis via DAPK2 and SQSTM1-dependent selective autophagy. Autophagy. 2016 Dec 1;12(12):2271–85.

106. Chi H-C, Chen S-L, Lin S-L, Tsai C-Y, Chuang W-Y, Lin Y-H, et al. Thyroid hormone protects hepatocytes from HBx-induced carcinogenesis by enhancing mitochondrial turnover. Oncogene. 2017 Sep;36(37):5274–84.

107. Perra A, Plateroti M, Columbano A. T3/TRs axis in hepatocellular carcinoma: new concepts for an old pair. Endocr Relat Cancer. 2016 Aug 1;23(8):R353–69.

108. Aranda A, Martínez-Iglesias O, Ruiz-Llorente L, García-Carpizo V, Zambrano A. Thyroid receptor: roles in cancer. Trends Endocrinol Metab. 2009 Sep 1;20(7):318–24.

109. Berkenstam A, Kristensen J, Mellström K, Carlsson B, Malm J, Rehnmark S, et al. The thyroid hormone mimetic compound KB2115 lowers plasma LDL cholesterol and stimulates bile acid synthesis without cardiac effects in humans. Proc Natl Acad Sci. 2008 Jan 15;105(2):663–7.